NADIA FATIHA RAMLAN B. ENG. (HONS) ELECTRICAL & ELECTRONIC ENGINEERING JANUARY 2017

OPTOELECTRONIC DEVICE FOR STRESS DETECTION

NADIA FATIHA BINTI A. RAMLAN

ELECTRICAL & ELECTRONIC ENGINEERING
UNIVERSITI TEKNOLOGI PETRONAS
JANUARY 2017

Optoelectronic Device for Stress Detection

by

Nadia Fatiha Binti Ahmad Ramlan

18115

Dissertation submitted in partial fulfilment of
the requirements for the
Bachelor of Engineering (Hons)
(Electrical & Electronic Engineering)

JANUARY 2017

Universiti Teknologi PETRONAS,
32610, Bandar Seri Iskandar,
Perak Darul Ridzuan.

CERTIFICATION OF APPROVAL

Optoelectronic Electronic Device for Stress Detection

by

Nadia Fatiha Binti Ahmad Ramlan
18115

A project dissertation submitted to the
Electrical & Electronic Engineering Programme
Universiti Teknologi PETRONAS
in partial fulfilment of the requirement for the
BACHELOR OF ENGINEERING (Hons)
(ELECTRICAL & ELECTRONIC ENGINEERING)

Approved by,

_____

(DR TANG TONG BOON)

UNIVERSITI TEKNOLOGI PETRONAS
BANDAR SERI ISKANDAR, PERAK
January 2017

CERTIFICATION OF ORIGINALITY

This is to certify that I am responsible for the work submitted in this project, that the original work is my own except as specified in the references and acknowledgements, and that the original work contained herein have not been undertaken or done by unspecified sources or persons.

_____

NADIA FATIHA BINTI AHMAD RAMLAN

ABSRACT

This research study aims to develop a portable, non-invasive stress monitoring system that uses near-infrared light which enables the recording of brain activities during the actual life experience memory task of a subject. This is to clarify the neurophysiological mechanism of stress response by identifying the local hemodynamic changes in human brain. Recent studies have shown that the stress response system able to influence the front part of the brain known as prefrontal cortex. In this paper, a non-invasive near-infrared spectroscopy (NIRs) technology is being studied to design a basic concept of photometric system that allows to monitor and imaging blood oxygenation through skin tissues. The proposed system is applied to human hands as proof of concept. The idea is to ensure that the photometric system can be applied at the forehead area where the level of oxygenation is expected to be higher at rest under mental stress condition. The data will be evaluated as well as the measurement and calculation made by illuminating the right wavelength towards the tissue and detects the reflected light, enabling spatially resolved spectroscopy to be carried out.

ACKNOWLEDGMENT

The author would hereby like to express a profound sense of gratitude to Associate Professor Dr. Tang Tong Boon for providing a good guidance to let the author understand the electrical knowledge in biomedical field. It is a great honor to have Dr. Tang Tong Boon as the supervisor for this project. Being part of this project has led the author to gain some knowledge and understand the connection of what electrical engineering able to offer in a real medical world.

Special thanks to the technicians from the electrical department who have given their cooperation and lend various essential components during the design process. However, this project would not have been complete without the help of Mr. Lim Lam Ghai for his amazing knowledge in circuit analysis that helps to run the system. To have been able to go through multiple research papers, the author is exposed virtually on how working alongside the professional researchers and engineers can be very tough especially when the research study can take up to more than a year.

All the tasks that is involved throughout developing this project have brought the author to experience technical skills and preparation of technical writings. Finally, a deepest appreciation to the author's family for their invaluable help of constructive comments and moral support throughout experiencing this project.

TABLE OF CONTENT

CHAPTER 1	**INTRODUCTION**	**PAGE**
1.1	Overview	1
1.2	Research Background	1
1.3	Objectives	4
1.4	Scope of Study	4
1.5	Problem Statements	5
CHAPTER 2	**LITERATURE REVIEW**	
2.1	Overview of Literature Review	6
2.2	Stationary FNIRs Experimented in Laboratory	6
2.3	Mobile FNIRs Experimented Outside Laboratory	8
2.4	Light Source	10
2.5	Light Detector	11
2.6	Portable and Light Weight Device	12
2.7	Pulse Oximeter	13
2.8	Blood Oxygen Saturation	16
2.9	Summary	17
CHAPTER 3	**METHODOLOGY**	
3.1	Overview of Research Methodology	18
3.2	Instrumentation Requirements	19
3.3	Hardware Development	20
	3.3.1 Microcontroller	20
	3.3.2 Light Emitter and Photodiode	21
	3.3.2.1 Light Source	21
	3.3.2.2 Light Detector	22
3.4	Software Development	24
	3.4.1 NI Multisim Circuit Simulation	24

3.4.2 EAGLE 7.7.0 Schematic Circuit Diagram 25
3.4.3 Programming Interface 26
3.5 Summary 27

CHAPTER 4 RESULT AND DISCUSSION

4.1 Overview of Result and Discussion 29
4.2 Discussion of Result 29
4.3 Estimation of SpO_2 Percentage 33
4.4 Summary 34

CHAPTER 5 CONCLUSION AND RECOMMENDATION

5.1 Overview of Conclusion and Recommendation 35
5.3 Conclusion 36
5.3 Recommendation 37
5.3.1 Realistic Brain Phantom (Future Work) 37

REFENRENCES
APPENDIX

LIST OF TABLES

TABLE NO.	TITLE	PAGE
2.2	: NIRs imaging application conducted in lab	6
2.3	: Table 2.3: Real world test using a portable NIRs system	8
3.3.2.1	: Features of red and infrared LED based on datasheet	21
3.3.2.2	: Features of photodiode based on datasheet	22

LIST OF FIGURES

FIGURE NO.	TITLE	PAGE
2.3	: Characteristic of lights from LED compare to laser	10
2.5	: Avalanche photodiode	11
2.6	: Example of a portable NIRS device used for experimentation purpose	12
2.7.1	: Clip-type probe of a standalone Pulse Oximeter	13
2.7.2	: Absorption spectra of oxygenated hemoglobin (HbO2) and deoxygenated hemoglobin (Hb)	14
2.7.3	: Transmission(left) and Reflectance(right) of light	15
2.8	: HbO2 absorbs more infrared lights and let the red pass through whereas Hb absorbs more red lights and let the infrared pass through.	16
3.2	: Processing section of oximeter	19
3.3.1	: Arduino UNO board(left) and ATMEGA328 pinout schematic(right)	20
3.3.2.1	: Infrared LED and Red LED	21
3.3.2.2	: SFH225 Photodiode	22
3.3.3.1	: LM324N Quad Operational Amplifier	23
3.3.3.2	: Testing circuit on breadboard	23
3.4.1	: Circuit simulation of Charge Pump	24
3.4.2	: Amplifier circuit	25
3.4.3.1	: Arduino Sketch	26
3.4.3.2	: Sample of output using Processing software	27
4.2.1	: Circuit simulation of Charge Pump	29
4.2.2	: Output signal of amplifier at 1.5kHz	30
4.2.3	: Output displayed using Serial Monitor	31
4.2.4	: Output displayed using Serial Plotter	31
4.2.5	: Output displayed after a few attempts	32
4.2.6	: Simulation of pulsatile flow in arteries	33

5.3.1 : NIRs application tested on a brain phantom 37

LIST OF ABBREVIATIONS

ADC	Analog-to-Digital Converter
AFE	Analog Front End
DAC	Digital-to-Analog Converter
Hb	Hemoglobin
HbO2	Oxygenated Hemoglobin
LED	Light Emitting Diode
MCU	Microcontroller Unit
PCB	Printed Circuit Board
PPG	Plethysmography
TIA	Transimpedance Amplifier
SpO2	Oxygen Saturation

CHAPTER 1
INTRODUCTION

1.1 Overview

This chapter provides detail review of a research study on the development of mental stress measurement system using the Near-Infrared light spectroscopy (NIRs) to measure the concentration changes of oxy-hemoglobin and de-oxy-hemoglobin which relates to detecting stress activities in brain. The purpose of this research paper is to propose a cost-effective and an alternative fast response method of portable system in studying functional activity during an actual real life experience which is more accurate compared to lab-based tests. The detailed background study and problem statement that leads to the objectives of the research are discussed under this chapter.

1.2 Research Background

Stress can be defined as a state of mental tension as the brain response to the feedback of the body and mind due to harmful situation or any environment that is under pressure. When the body felt threaten, it will automatically rouse itself for emergency action. Thus, this will speed up the heart rate, breathing heavily, increases the blood pressure and boost the amount of energy to the muscle. Stress can be healthy if it is short-lived. However, if the stress is excessive or uncontrollable, it can affect one's emotion which may leads to mental illness as well as physical health. It does not only cause by external factors, instead, it can also be internal or self-generated such as worrying excessively about something, solving calculations during exam or even lack of sleep causing the brain to have insufficient oxygen. Oxygen deficiency will lead back to mental stress which in advance causing brain cells to damage slowly. Whether the stress is physical or mental, the response is still the same**[20]**.

Stress can be measured according to behavioral and physiological responses. There have been wide-ranging questionnaires that have been developed to assess the psychological factors that are linked with human stress**[1]**. However, this method is not precise enough to determine the level of stress in human. The irregularity of function within the frontal part of the brain can be difficult to distinguish in the lab or clinic as it is located under the skull**[2]**. Nevertheless, to recreate the test in lab could be less favorable since the participant can change their behavior in a way that the body is prepared and ready to approach task given since they are aware of the situation**[2]**.

Recent studies have shown that the optical measurement technologies in imaging are emerging rapidly towards the medical applications**[3]**. The technology used is to study tissue structures by analyzing scattering lights and the absorption of hemoglobin. Near-infrared (NIR) light can passes through the skin, scalp and skull with a small percentage of the amount of power per unit volume which are able to reach the prefrontal cortex of human brain**[4]**. It has become the alternative quick response in analyzing the brain activities.

Near Infrared-light spectroscopy (NIRs) is an effective tool to identify the characteristic of the prefrontal cortex in emotional processing**[5]**. It is used for non-invasive assessment in biomedical technology such that it measures the functionality of brain and other tissues as well as an analytical tool for diagnosing disease**[6]**. This technology is mostly used in laboratory testing for various pharmaceutical applications. These many elements are impossible to detect with the human naked eye, thus, with this spectrophotometer technology it will use the reflectance of lights and absorption values to quantify the data to help accurately detect impurities and classify materials.

Near-infrared spectroscopy (NIRS) is widely known for its optical monitoring technique that derives the concentration changes of oxygenated and deoxygenated hemoglobin**[7]**. Pulse oximetry is a based technique of near-infrared (NIR) light which has been widely used to detect the arterial blood saturation under the skin for clinical practice**[3]**. When the absorption spectrum of light is analyzed, the measurement of that light intensity can be used to determine the concentration of blood and tissue oxygenation which demonstrates the local hemodynamic responses. The oxygenated and deoxygenated hemoglobin molecules can be found in cerebral tissue. The measurement of cerebral blood flow offers extremely useful information especially for patients who are related to neurological disorder.

Now, people are moving forward to providing a portable stress monitoring system to experience a real-world test in a normal people's life and activity as it is said to be more accurate and precise study in human stress**[8]**. The idea is to undergo the imaging techniques on the forehead area where the concentration of blood oxygenation is known to be very high while freely encountering the on-going daily activity. Hence, it is important to understand the basic method of measuring the blood concentration through skin. Besides having a unique idea of a portable imaging system, it can also affect the cost of developing the device in a way that the usage of opto-mechanical coupling components and fiber-optics will be replace with a cheaper component with almost the same outcome**[8]**. Furthermore, the hardware design itself should be less complex to reduce the overall instrument size and weight. Thus, this will make it more convenient for the subject to move around compare to the existing NIRs machines in the lab.

1.3 Objectives

The objectives of research were described as follows:

- To propose a cost-effective optoelectronic device that can be used to measure the blood oxygenation in determining the hemodynamic response which indirectly reflects the functional neural activities in human brain.
- To design and integrate a single channel of NIRS system in order to understand the basic concept of NIRs technology.

1.4 Scope of Study

The research study focuses on as described below:

1. Biomedical information of functional brain studies affected by stress response.
2. The development of instrumentation for near-infrared spectroscopy and clinical research in translational of brain imaging.
3. The procedure of estimating blood concentrations in the absorptions of oxygenated and deoxygenated hemoglobin.
4. Different approaches of implementing the near-infrared spectroscopy in order to monitor tissue hemodynamics and oxidative metabolism.

1.5 Problem Statement

Near Infrared-light spectroscopy (NIRs) imaging system available on the market is very expensive now-a-days. The technology provides a valuable clinical purpose but due to its high cost development, it limits the accessibility to most patients out there. For an example, Hitachi ETG4000 is a common and an effective NIRs system that is used in most private hospitals. However, to purchase the machine can cost up to RM1 million at its minimum price. Besides the price itself, to prepare the treatment will need to encounter many wirings connections only for the head gear to the machine. This will constrain the patients to move freely. All of the treatments will be resulted depending on the lab-based test which will give an artificial result under the constrained testing environment. Thus, the measurement of mental stress provided by the analysis is based on the unnatural environment.

CHAPTER 2
LITERATURE REVIEW

2.1 Overview of Literature Review

This chapter will discuss on other similar applications of NIRs technology that employ either lasers or light emitting diodes (LED) as the light source considering situational factors from existing research papers and the study of instrumentation requirements to develop a basic photometric system. There will be a case study of theoretical oximetry equations related to finding blood oxygen saturation and the comparison of commonly used light sources in biomedical technology to aid the design specification for this research. Thus, the information discussed will provide a solid background of research and general understanding that should give meaning to the discussion of findings, conclusions, and recommendations. The determination of procedure used in past studies is identified and studied to clarify the theoretical framework before moving forward to methodological focus.

2.2 Stationary FNIRs Experimented in Laboratory

Table 2.2: NIRs imaging application conducted in lab

Paper	Diagnosis	Method	Type of FNIRS System used	Light Source
S. Pu, 2008**[26]**	Major Depressive disorder (MDD)	• VFT procedure • Vocalization effects	ETG-4000 Optical Topography System	Laser
G. Durantin, 2014**[25]**	Post-traumatic stress disorder (PTSD)	Computerized simulation	fNIR100 (Biopac®)	LED
S. Moghimi, 2012**[24]**	Emotional arousal response	Music-based emotion induction paradigm	ISS Imagent Functional Brain Imaging System	LED

M. Kawano, 2015**[3]**	Depression	Verbal Fluency Task	Twenty-two channel NIRS ETG-4000	Laser

The application of NIRs technology for brain imaging is usually handled safely in the laboratory where the subjective measures is assessed through questionnaires and there will be less movement for the subject. The idea is to record the brain function during the assessment to monitor cerebral oxygenation changes. The verbal fluency task has become a well-known assessment used to evaluate the prefrontal hemodynamic response**[2]** and to assess the relationship between activation in the prefrontal areas and clinical characteristics involving social functioning**[2]**.

According to Kawano's research paper, the procedure of handling the assessment will normally takes up to more than 15-20 healthy persons depending on age and gender. Each assessment is conducted at different timing so that to minimize the time during which the subject is stand still and remained silent**[2]**. On the other hand, Moghimi research paper used the NIRs technology to study the emotional arousal by identifying the hemodynamic response of PFC**[24]**. It is conducted by using the music-based emotion induction paradigm to 9 individuals without any known health condition. The recording of wavelet-based peak detection extracted from the hemoglobin concentration on PFC notably associates with emotional valence and arousal. However, these procedures are usually handled in bulky setups with multiple wirings connected from the head gear to the machine that may interfere subjects during assessment. Thus, it has a high risk of patient discomfort which will make it impossible to study the responses in real-life settings**[2]**.

Durantin's paper**[25]** has identified the pilot instantaneous mental state using a realistic flight simulator while having the NIRs brain imaging system to assess the working memory. The result offers a promising point of view towards the design of NIRs-based BCI for pilots. However, to be use in a real cockpit still endures a challenge as safety is prioritize in aeronautics. Hence, the result obtained is artificial as it is tested under unnatural events.

2.3 Mobile FNIRs Experimented Outside Laboratory

Table 2.3: Real world test using a portable NIRs system

Paper	Diagnosis	Method	Type of FNIRS System used	Light Source
C. Song, (2016)	Physiological effects	Walk in a street	NIRO-200NX	LED
B. Jones, (2016)**[28]**	Muscle and brain activity	Walk up 8 floors and back down	NIRO-100	Laser
T. Liu, 2015**[27]**	Mental stress	Presence of others (PO) affects	2-channel NIRS unit (PocketNIRS)	LED
P. Pinti, 2015**[2]**	Functional Brain activity, behavior	• Stand stationary • walk a short distance • walk around entire street area	Multichannel Wearable FNIR	LED

Recently, most researchers have move towards a portable and lightweight neuroimaging techniques that does not require significant physical restraints**[2]**. The idea is to study the brain activities outside the lab so that to experience the real-world test. Researcher known as Pinti found that having to test under real event can be more sensitive and accurate in assessing cognitive function compare to lab test. The subject is acquired to walk around while accomplish several different tasks like having a normal daily activity written in Song's research paper. According to Pinti, this allows the changes of blood oxygenation to occur within the walking period to monitoring the responses in brain function.

The data is measured over the prefrontal cortex with the portable NIRs device while the subject experiencing different task outside the lab. It is observed that the diagnosis involves walking by the road side, climbing up the stairs and the interactions with other subjects**[27]** where the behavior is self-initiated, such situations are difficult to recreate in the laboratory.

Every movement made to the body affected the muscles. More blood is pumped to the muscles during the walking period to deliver additional oxygen. Therefore, B. Jones**[28]** stated that considering physiological interventions with NIRs, allows quantitative measurement to be made from the muscles. Hence, the opportunity to study functional brain activity during real-world test has proven that the experiment conducted is natural and unrestrained settings. The data obtained is more accurate as it is not artificial compared to the lab-based test results**[2]**.

2.4 Light Source

Table 2.4: Specifications of light sources

	Light Source	Wavelength(nm)	Power	Type
Emitters	Ultraviolet	370	60mW	UV LED
	Red LED	660	100mW	Red LED
	Laser	685	20mW	Laser diode
	Infrared LED	940	85mW	IR LED

There are four different type of light source with each different wavelengths and power consumptions. These light sources are commonly used in biomedical technology. Most types of the light sources used are of the light emitting diode (LED). LEDs are proving to be more reliable, longer lasting, high efficiency and lower in cost compare to laser. LED emits incoherent narrow spectrum light. It can be more reliable and durable device oppose to laser. It is less invasive and safer to use. LED uses lower power densities and far lower current densities in which reduces the chance of stress limit in the material itself. Clearly, the power output optimized is to be most efficient and less risk compared to laser. Even though LED is much lower cost than laser, it can still delivers the same healing wavelengths as lasers**[4]**. However, how depth is the penetration of light does not affect the efficiency but rather related to energy density and the wavelengths.

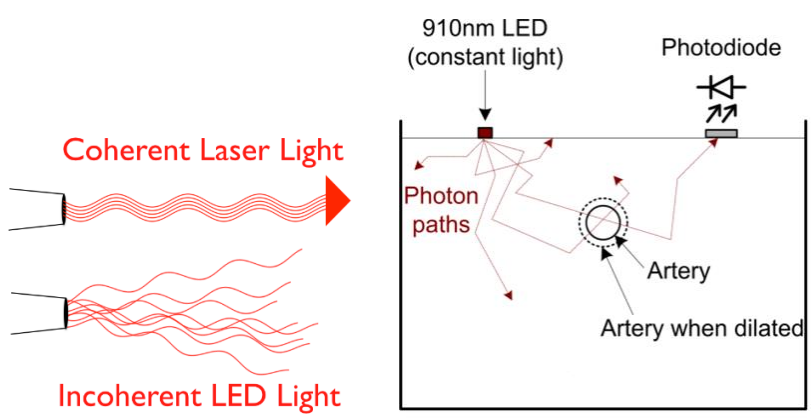

Figure 2.3: Characteristic of lights from LED compare to laser.

2.5 Light Detector

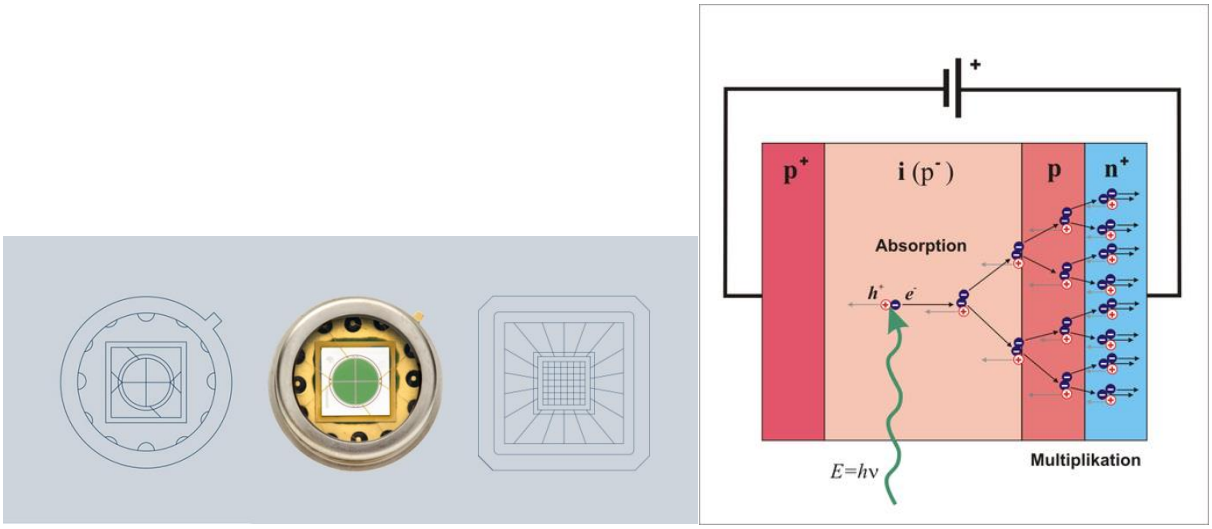

Figure 2.5: Avalanche photodiode

Silicon Avalanche Photodiodes (APDs) are highly sensitive semi-conductor running at a high speed for "light" sensors. APD have an output with a superior signal-to-noise ratio (SNR) compare to what can be obtained with conventional photodiode. It is a type of photodiode that has a large reverse bias voltage applied to it. While operating under the high reverse bias condition this will allow the initial hole electron pairs created by the photons to generate avalanche multiplication of holes and electrons. Since the gain level increases when higher voltages are applied, the gain of these avalanche diodes will cause a greater level of sensitivity of the photodiode**[4]**. Signal amplification within the photodiode is generated due to the large electric field which allows much higher quantum efficiency. Normally the signal is amplified within the device, thus it can measure lower level light and be used in any applications that require high sensitivity**[4]**. APD can detect light with the wavelengths of 300 to 1600nm.
However, it is also depending on the material used as some is manufactured to detect wavelengths up to certain micrometers.

2.6 Portable and Light Weight Device

Figure 2.6: Example of a portable NIRS device used for experimentation purpose

While most neuroimaging techniques portrays a powerful tool to monitor brain function in a non-invasive way, it is inappropriate to impose physical constrain to the subject for use in everyday life setting**[2]**. Thus, this has encouraged the researchers to improve the technological imaging system given the need to bring functional imaging instrument outside the lab. Portable NIRS imaging system opens up a new point of view towards the study of cognitive paradigms in the realistic environments. Same goes to the wireless EEG imaging system which shows the evidence of stability in real-world measurements whereby it is able to measure the function of cerebral oxygenation outside the laboratory**[9]**. The idea has given a room for new desirable applications in biomedical technology.

2.7 Pulse Oximeter

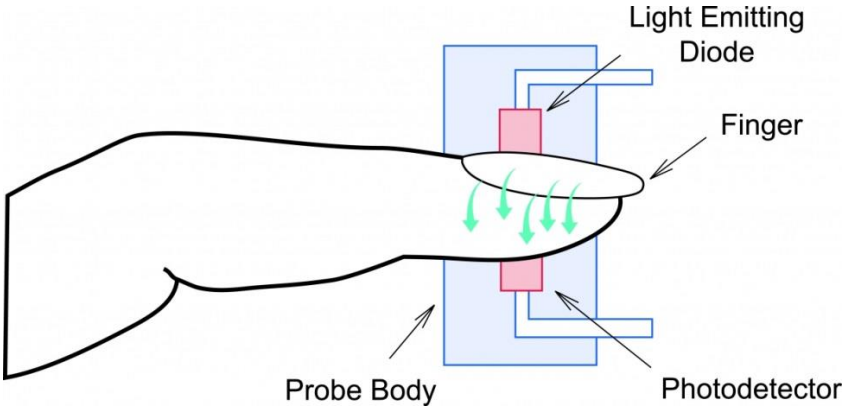

Figure 2.7.1: Clip-type probe of a standalone Pulse Oximeter

Pulse oximetry is a fundamental non-invasive technology in biomedical field. It monitors oxygenation of hemoglobin based on the measurement of arterial oxygen saturation (SpO_2)**[10]** which can be detected from certain parts of the body such as wrist, ear lobe or forehead. Measurement of these blood components provides an advantage to monitor brain activities as well. It consists of light emitter flashing alternately through the skin allowing the absorption of light from blood and photodiode to capture the reflected light**[11]**. The arterial oxygen saturation (SpO_2) allows us to determine the health condition of a patient. A healthy patient will usually be in the range of 94% to 99%**[12]**. If the oximeter detects less than 90%, thus, it indicates the patient has insufficient supply of oxygen in their body.

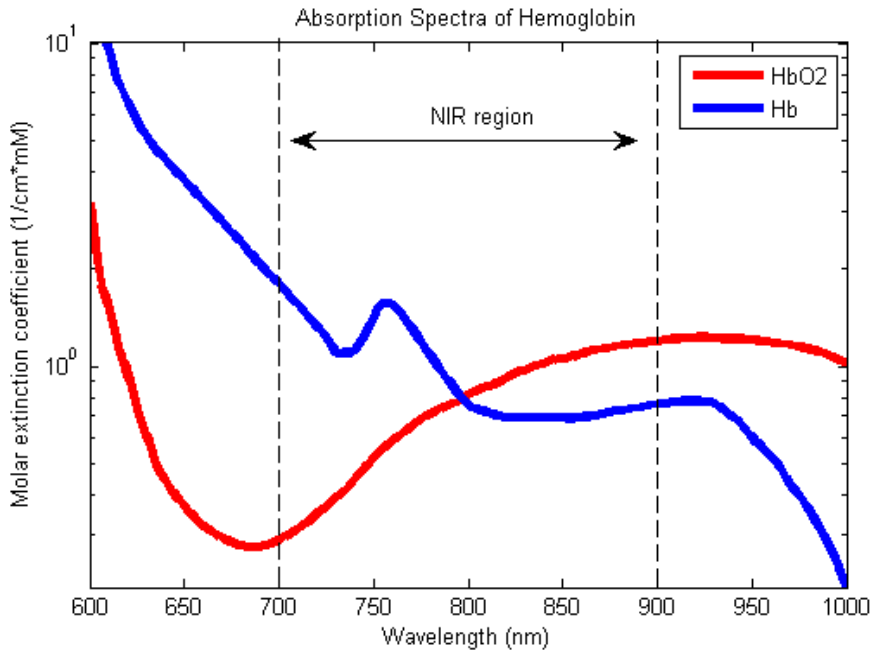

Figure 2.7.2: Absorption spectra of oxygenated hemoglobin (HbO2) and deoxygenated hemoglobin (Hb)

Pulse oximeter uses light emitter with red and infrared LED to detect Oxygenated (HbO2) and Deoxygenated (Hb) blood to determine the SpO_2. The Oxygenated and deoxygenated blood both have different absorptions at different wavelength as shown in **Figure 2.7.2**. Oxygenated hemoglobin absorbs more infrared light with wavelength between 850-1000nm of light band whereas deoxygenated hemoglobin absorbs more red light in 600-750nm wavelength of light band**[12]**. The oximeter will only function when it detects a modulation in transmitted light. Therefore, if perfusion is weak and the pulse amplitude produced is small, it will lead to error or fail to obtain a reading.

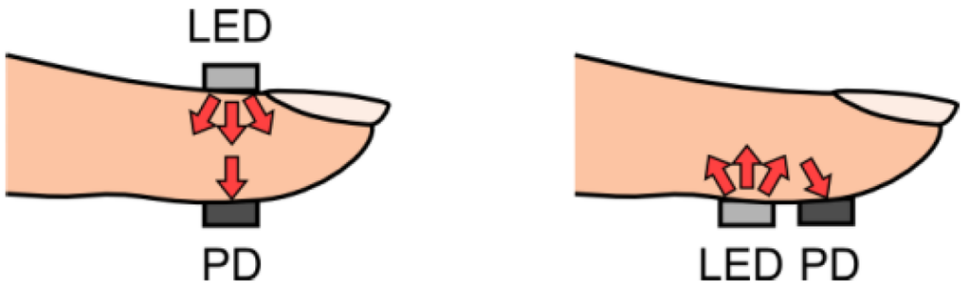

Figure 2.7.3: Transmission(left) and Reflectance(right) of light

There are two ways of transmitting light through the site being measured which is reflectance and transmission. Transmission method is the measurement in-between site whereby the photodiode and emitter are opposite of each other allowing the light passing through the site. However, for the reflectance method, the light source and photodiode is mounted next to each other underneath or on top of the site. This will cause the light to shine and bounces back to the detector across the site. In most hospital, transmission pulse oximetry is an efficient method in monitoring SpO_2 in neonates and adults**[13]**.

There have been several publications described the theory of conventional pulse oximetry **[14]**. The signal curves of Photoplethysmography (PPG) is due to the changes of blood concentration which gives the measurement of light absorption; based on the two wavelength and the blood oxygen saturation is derived from the ratio**[15]** which is defined by:

$$\boldsymbol{Ratio}\ (\boldsymbol{R}) = \frac{\left(\frac{\boldsymbol{AC_{red}}}{\boldsymbol{DC_{red}}}\right)}{\left(\frac{\boldsymbol{AC_{infrared}}}{\boldsymbol{DC_{infrared}}}\right)} \qquad \textbf{(1)}$$

whereby DC and AC are the baseline of the pulse and the peak-to-peak amplitude. A logical relationship between oxygenation saturation and the ratio of modulation pulse can be identified by applying the Lambert-Beer Law and study of the light absorption and scattering in tissue that includes blood (Hb and HbO2).

2.8 Blood Oxygen Saturation

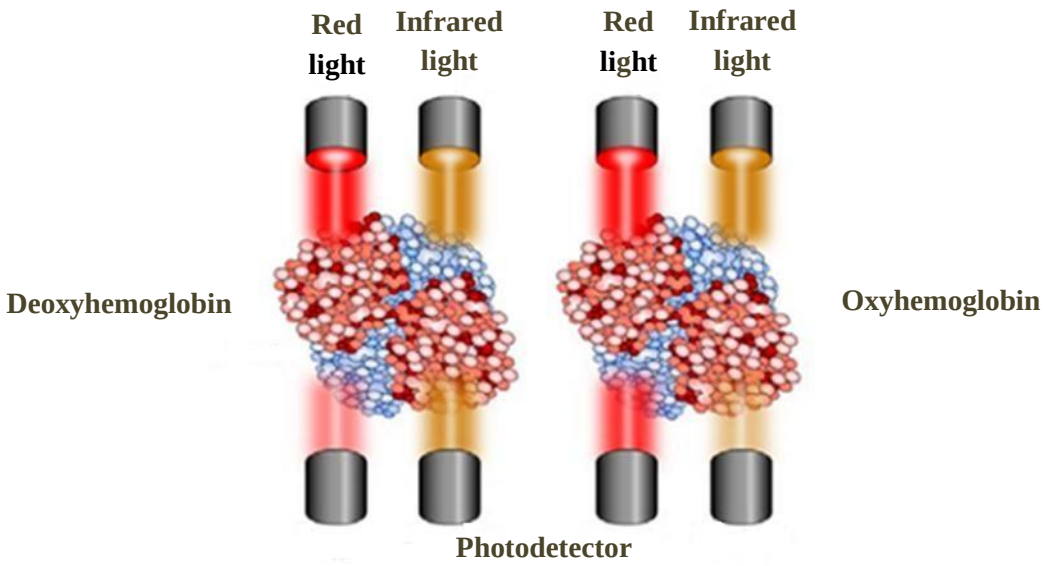

Figure 2.8: HbO2 absorbs more infrared lights and let the red pass through whereas Hb absorbs more red lights and let the infrared pass through.

Blood oxygen saturation can be identified by examining hemoglobin. Hemoglobin is known as the oxygen-carrying-protein in human blood. The blood is fully oxygenated when the hemoglobin carries a maximum number of oxygen molecules. However, as the hemoglobin releases oxygen molecules to the tissue, thus, causes the blood to become deoxygenated. The saturation of blood oxygen can be determined by measuring both Oxygenated (HbO2) and Deoxygenated (Hb) hemoglobin**[16]** by shining a red LED and an infrared LED through the skin and then compare its relative intensities. The absorption of oxygenated blood and deoxygenated blood from the light source can be observed in **Figure 2.8**. To measure the hemoglobin saturation, there must be two wavelengths of Hb and HbO2, thus, the equation can be derived as:

$$\boldsymbol{SaO_2 = \frac{HbO_2}{Hb + HbO_2}\, x\, 100\%} \qquad \textbf{(2)}$$

The above definition is referred to as functional hemoglobin saturation. The other two hemoglobin species, Methemoglobin and Carboxyhemoglobin is ignored as it does not contribute to functional oxygen support**[16]**.

2.9 Summary

The previous research papers have helped to give the idea and guidance to support the next step of research methodology. The IR LED has been the best option as a non-invasive light source that can be used to design the photometric system alongside the photodiode. The idea of using the amplifier and filter is the simplest method to improve the signal before sending it to the microcontroller. The conversion of signal to digital can be done by the microcontroller to use it to calculate the data and at the same time it can be used to control the pulsation towards the LED driving circuit. The finger is chosen as it is more direct and smaller surface area, thus, it is easier to make a measurement. The literature review has elaborated important knowledge and the overview on how the design of this project should look like throughout this research process. Thus, the methodology will briefly discuss on the design specification of this prototype.

CHAPTER 3
METHODOLOGY

3.1 Overview of Research Methodology

The design specification of this research is at the early stage of designing phase where the idea is to get a better understanding on the basic concept of NIRs imaging techniques. This is done by building a simple sensing mechanism into the system that able to detect light absorption from tissue to determine the changes in the concentration of oxyhemoglobin. Transmission method is used for the design of the photometric system where the LED and photodetector are opposite of each other with the measuring site in-between. The device is a single channel system that uses signal conditioning and filter out the signal from the photodiode before converting it to digital output for data analysis. The idea of making the device portable, a battery of 9v is used to power up the oximeter once the design is complete. There will be a programming interface involved to control the pulsation and command from the microcontroller. The research methodology applied is purely based on the case studies made in literature review.

3.2 Instrumentation Requirements

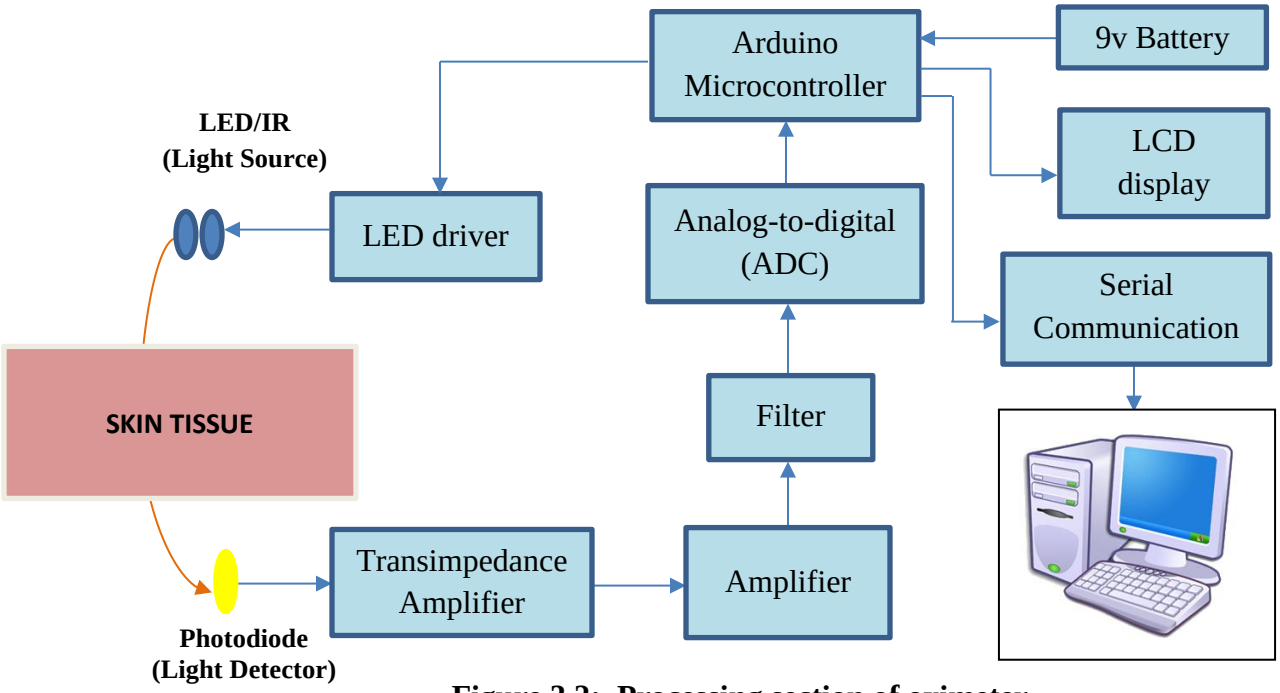

Figure 3.2: Processing section of oximeter

Based on the literature review, the system is divided into three modules which are the pad to hold the sensors and the light source, a control box for hardware management and a process unit that stores data. The light source is transmitted using light emitting diode (LED) which will penetrate through the skin and absorbed by the tissues at two different wavelengths (660 and 940nm). LED driver circuit is designed to drive each wavelength separately. Each different wavelength is used to measure oxy-hemoglobin and de-oxy-hemoglobin. The transmitted IR signal that managed to penetrate through the skin is reflected by the blood cells. The photodiode will be used to detect the reflected light and converts the current output to voltage value using a current to voltage converter. The signal will be amplified, filtered by the LM324N IC before feeding it to the microcontroller for further data processing. The excellent part of it is that the Arduino Uno board is built in with ADC channels. Thus, the microcontroller reads the analogue value and convert this signal to digital value. The 9v battery and LCD display is mounted to portray the portability of the device. However, for the testing purposes, serial monitor will be used temporarily until the right data is obtained.

3.3 Hardware Development

3.3.1 Microcontroller

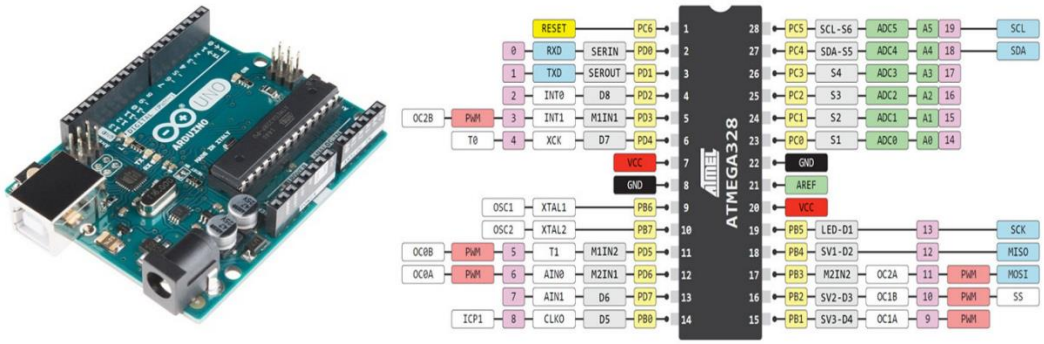

Figure 3.3.1: Arduino UNO board(left) and ATMEGA328 pinout schematic(right)

The Arduino hardware is used to control the system by sending the timing signals or pulse to ensure that the sampling is performed at the correct timing. It can be powered up via USB connection or with an external power supply. The external power source can come either from an AC-to-DC adapter or a battery. Arduino board is known as an open source platform consists of a programmable microcontroller with I/O pins. To build an oximeter, the board will be used and programmed with the Arduino software and evaluate the data obtained by the photodetector. The goal is to command the board to convert the signal into digital and measure the oxygen saturation before sending the output to display monitor. On the other hand, the pulse from microcontroller will switch the LEDs on and off, allowing the photodiode to measure the absorbance of light at both wavelengths independently.

3.3.2 Light Emitter and Photodiode

3.3.2.1 Light Source

Figure 3.3.2.1: Infrared LED and Red LED

There are two types of light emitter that will be used as the photometric system which is red and Infrared LED. The light emitter is based on two different wavelengths due to the absorption of two different type of hemoglobin. The value of extracted arterial oxygen saturation (SpO_2) that is corresponding to the oxygenation of the arterial bloods, is defined by the ratio of the pulsatile part using these two wavelengths**[17]**. The range of wavelength for the red LED has to be between 600nm to 700nm whereas for the infrared LED is b 850nm to 1000nm. Both the material is made up of Aluminium Gallium Arsenide (GaAlAs). Table below are the features for both LED:

Table 3.3.2.1: Features of red and infrared LED based on datasheet

	Red LED	**Infrared LED**
Wavelength	660nm	940nm
Forward Current	155mA	200mA
Forward Voltage	2.5V	1.6V
Radiant Intensity	75mW	80-400mW
Storage Temperature	-40°C to +85°C	-40°C to +100°C

3.3.2.2 Light Detector

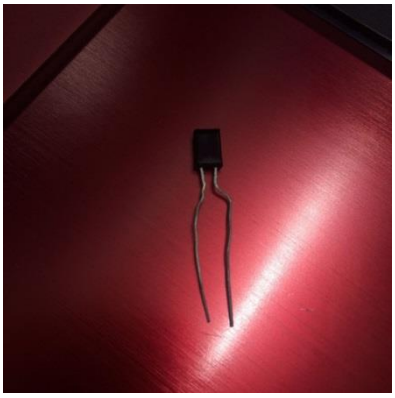

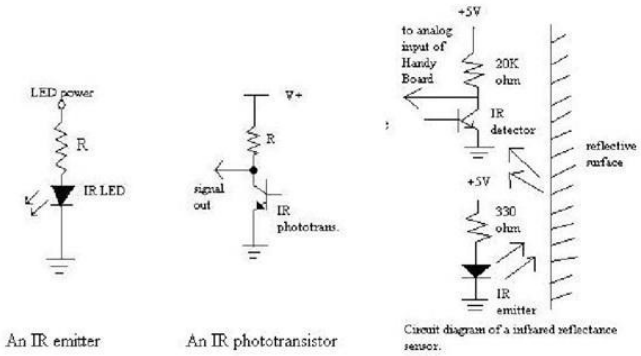

Figure 3.3.2.2: SFH225 Photodiode

Photodiode is an input device that should have a broad range of spectral responses that overlap emission spectra from both LED. The current produced by photodiode is directly proportional to the intensity of light emits. The photodiode should detect the light reflected from the skin. However, it fails to differentiate red or infrared light if both emit at once. Thus, in order to accommodate this, the microcontroller system should alternately turn each LED on or off. To enhance the quality of the Plethysmography, the suitable technique is by placing the photodiode close to the LED. Table below are the features of photodiode:

Table 3.3.2.2: Features of photodiode based on datasheet

	SFH225 FA
Wavelength	880nm
Forward Current	-
Forward Voltage	1.3V
Radiant Intensity	75mW
Storage Temperature	-40°C to +80°C

3.3.3 Circuit Connection

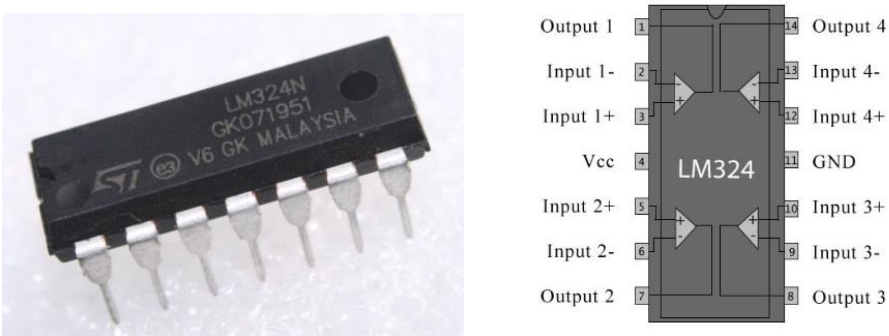

Figure 3.3.3.1: LM324N Quad Operational Amplifier

LM324N is a low power quad operational amplifier consists of four independent, high-gain, internally frequency which is designed to operate from a single power supply to a wide range of voltages. The connection is tested using a simulation with other components connected to it. This simulation can be observed under the Software Development section.

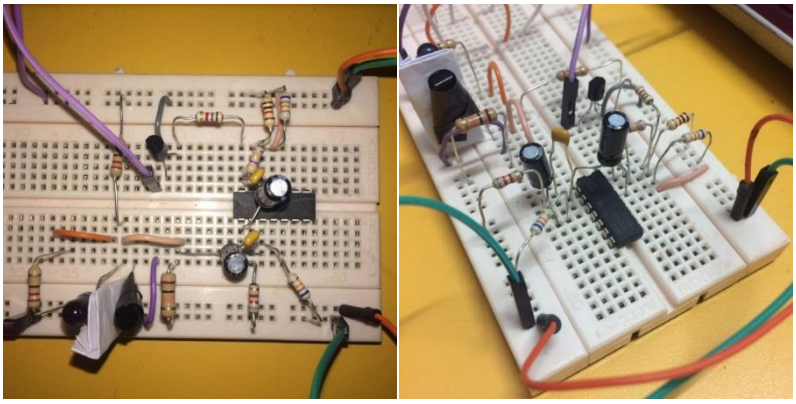

Figure 3.3.3.2: Testing circuit on breadboard

Circuitry connection is tested using breadboard before solder it to PCB. It is a great tool for easy prototyping. The purpose is to build and test an early version of electronic circuit. The connections are not permanent, thus, making it easy to remove a component or start over with different connections. As seen in **Figure 3.3.3**, the amplifier circuit is build using the amplifier to achieve a steady baseline for the signal. For the photometric sensors, it is separated with a white paper in between the LED and the photodiode to get a better reading of reflected light. This

board runs at 5v with the Arduino microcontroller. However, this circuit connection is just the early stage of developing the prototype. There will be more connection needed in order to complete the circuit design.

3.4 Software Development

3.4.1 NI Multisim Circuit Simulation

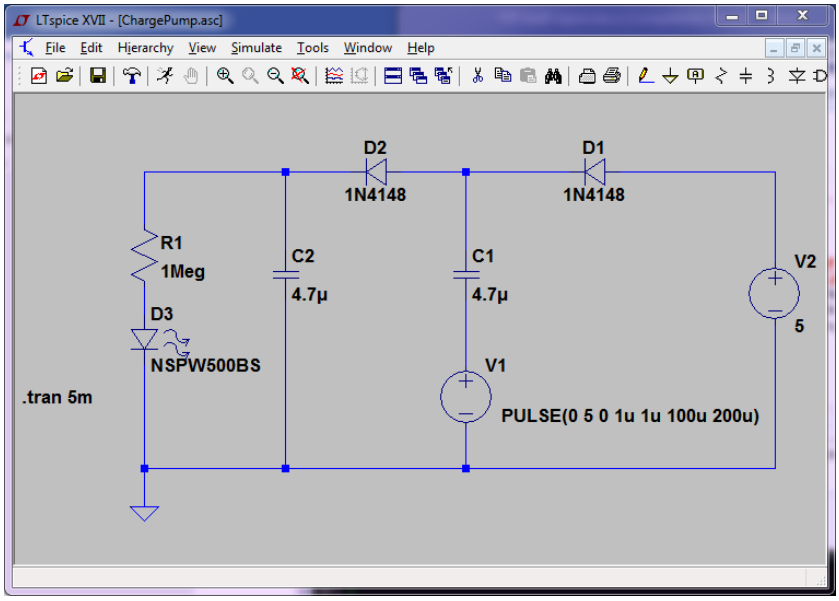

Figure 3.4.1: Circuit simulation of Charge Pump

5V-supply from Arduino is not enough to drive the LED. Thus, the purpose of having this circuit is to boost**[18]** DC voltage up to 8V. It works like LED circuit driver whereby it helps to enhance the light intensity of the LED. The red LED typically has higher forward voltage. Some of it can go up to 4V. The photodiode needs to detect enough light to give an accurate reading for the concentration of the hemoglobin. Hence, LED driver circuit is needed to provide the LED with ample energy to work.

3.4.2 EAGLE 7.7.0 Schematic Circuit Diagram

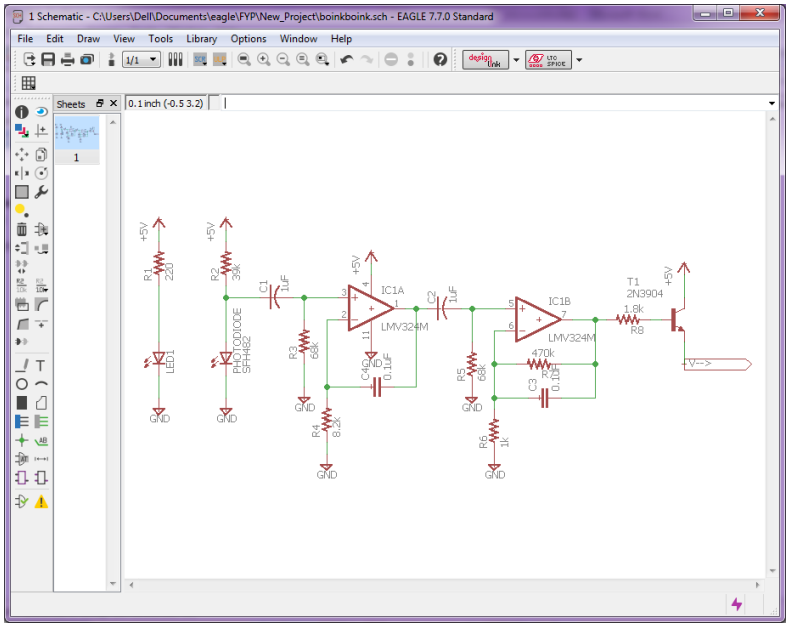

Figure 3.4.2: Amplifier circuit

The infrared LED and Photodiode is mounted opposite of each other to apply the transmission method. The IR emitter will emit an infrared light through transmission and the light detector will measure the amount of infrared light that gets reflected back. The more light is detected, the higher the current that pass through the detector. Hence, giving it a voltage drop as it enters the amplifier circuit. The circuitry design uses two operational amplifiers to demonstrate a steady baseline for the signal, filter out noise and emphasize the peaks. Both op-amps can be found in the IC of LM324N. Once the schematic circuit is done, it is just a matter of connecting the pins correctly to the breadboard for further testing. The amplifier output signal is then displayed using Processing 3 software by connecting the circuit from Arduino to a display monitor.

3.4.3 Programming Interface

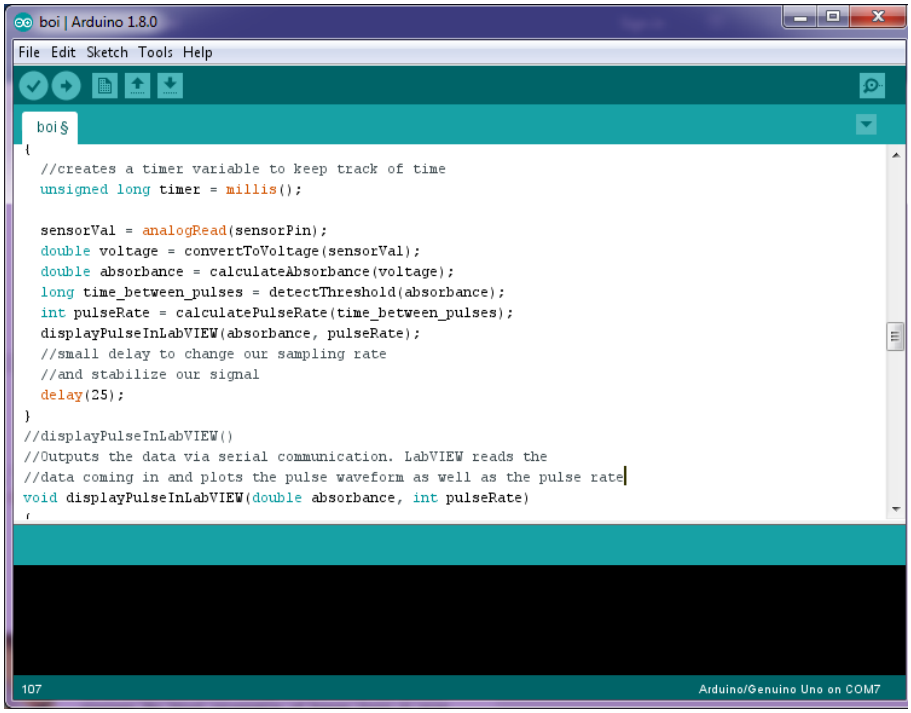

Figure 3.4.3.1: Arduino Sketch

Arduino IDE (Integrated Development Environment) is used to write a program and upload it to the board to give a command. The result can be viewed using a serial monitor. The program for Arduino is called a sketch which can be compiled and uploaded directly to the board. Based on **Figure 3.4.3.1**, the Arduino is programmed to display the behavior of the sensors whether it detects the present of the skin or not. The programming code is attached in **APPENDIX A**.

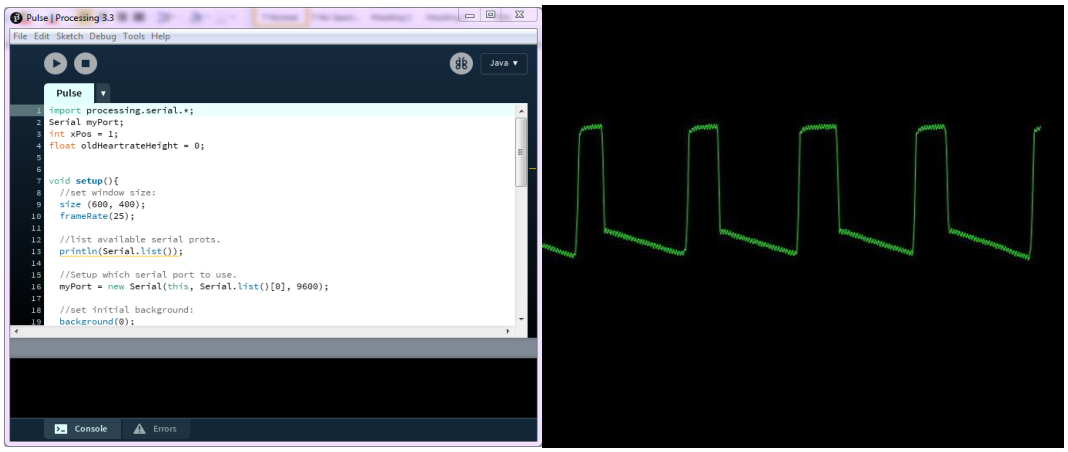

Figure 3.4.3.2: Sample of output using Processing software

The Processing software is used to display and graph the output of signals command by Arduino to the board. It works like oscilloscope in displaying the graph signal. Graphing value is useful to detect the component's behavior. The codes are used to communicate with Arduino by allowing processing sketch to read the data from Arduino's serial port. The programming code is attached in **APPENDIX B.** As shown in **Figure 3.4.3.2**, the right image shows the pulse signal detected from the sensors.

3.5 Summary

The research methodology has discussed mainly on the design specification and the development of the oximeter in terms of hardware and software. The sensing system is designed such that the measuring site is placed in between the light source and light sensor. This method is called transmission method as it is more efficient and easier for the light sensor to detect the reflected light. A charge pump is implemented as the LED driver to enhance the brightness of the LED and boost up to 8-9v safely. This will efficiently allow more light passes through the tissue and reflected back to the light sensor. The more light is detected, the higher the current passes through the photodiode. The reflected light that is detected by the light sensor is convert to voltage using a current to voltage converter. The signal will continually be amplified and filtered by LM324N quad op amp that can work in dual supply mode. The circuitry of the amplifier can be observed in **Figure 3.4.2**. This is to achieve a steady baseline for the signal, emphasized peaks and noise filtered. The signal will transfer to the Arduino microcontroller and converted from analogue to digital signal. This will then display to the serial monitor for further data analysis. At

the early stage of designing, the circuit connection is first tested using the simulation software before mounting it to the breadboard and secure the connection on PCB.

Programming interface is the tricky part of the design process. The C source code is modified to program the microcontroller in order to do some calculation and data conversion so that the oxygen saturation result can be obtained. During the testing, the result is viewed on the serial monitor and threshold value is adjusted based on the result obtained until the graph is displayed correctly. For future work, there will be more adjustment to the coding to determine the changes of oxygen saturation which indirectly reflects the functional neural activities in brain.

CHAPTER 4

DISCUSSION OF RESULT AND FUTURE WORK

4.1 Overview of Result and Discussion

This chapter will explain the result obtained throughout the research. The discussion will include problems encountered during testing on other similar applications of NIRs technology that employ either lasers or light emitting diodes (LED) as the light source considering situational factors from existing research papers and the study of instrumentation requirements to develop a basic photometric system.

4.2 Discussion of Result

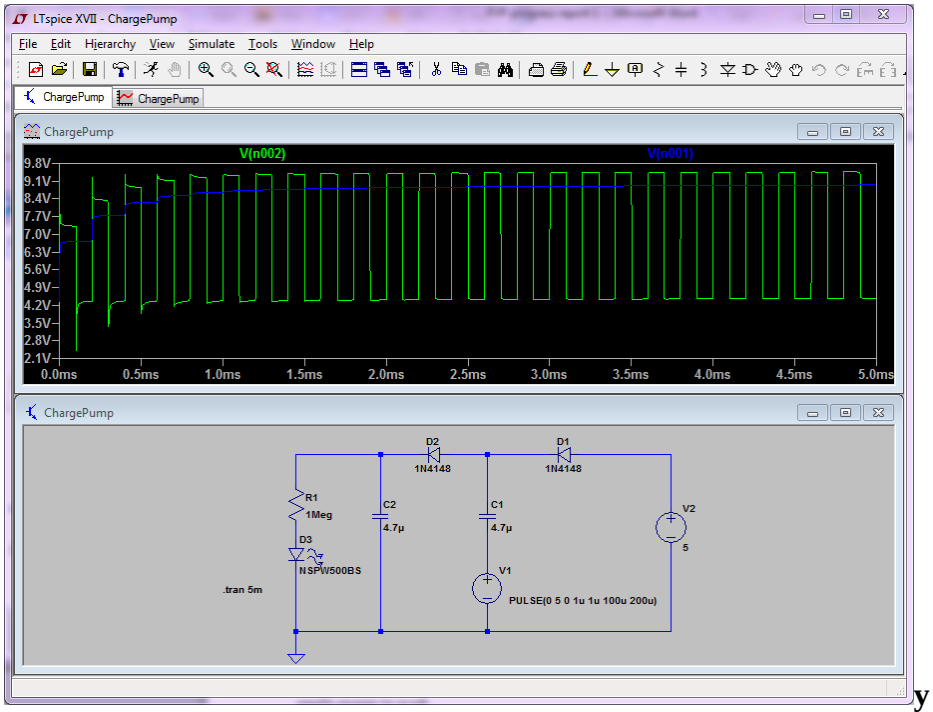

y

Figure 4.2.1: Circuit simulation of Charge Pump

Figure 4.2.1 gives the view of a working charge pump. Based on the basic principle of charge pump, the first stage of capacitor, C1, (which is the green line) will charge up to 5V if neglected the diode. Then, charge from C1 moves to C2, charging to 5V. Total up the voltage from both of the cascade will give the output voltage around 10V to be exact. shows that will first charge until it reaches 5vthen the Higher frequency and bigger capacitor pumps up the output but it will

never go beyond the theoretical limitation. When the load is removed, theoretical output voltage is approximately 9v. This is based on the calculation:

$$\boldsymbol{Vout = (N+1)(V_{cc}) - N\left(\frac{(I_2)(T)}{C}\right) - (N+1)(V_f)} \qquad \textbf{(3)}$$

$\boldsymbol{N}$ is the number of stage. $\boldsymbol{V_{cc}}$ is supply voltage of 5v (from the Arduino) whereas $\boldsymbol{V_f}$ is the diodes' forward voltage or diode voltage drop typically about 0.5V. The middle equation which is $\boldsymbol{N\left(\frac{(I_2)(T)}{C}\right)}$ is the loss term that must be considered**[19]**. If load is added to the circuit, thus, the output will go slightly lower. Thus, charge pump is a useful DC to DC converter that uses capacitors in promoting high bias voltages from a single low-voltage supply.

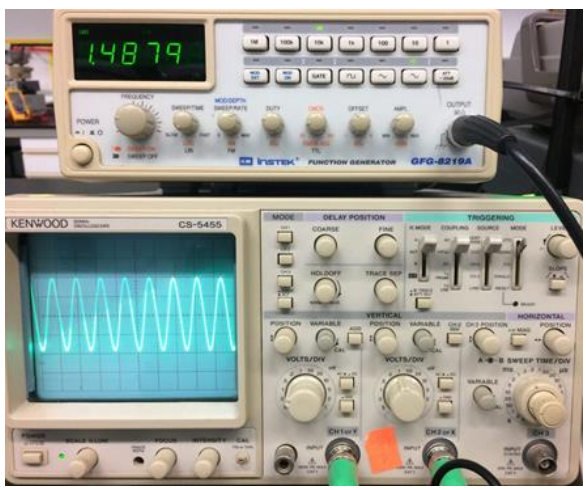

Figure 4.2.2: Output signal of amplifier at 1.5kHz

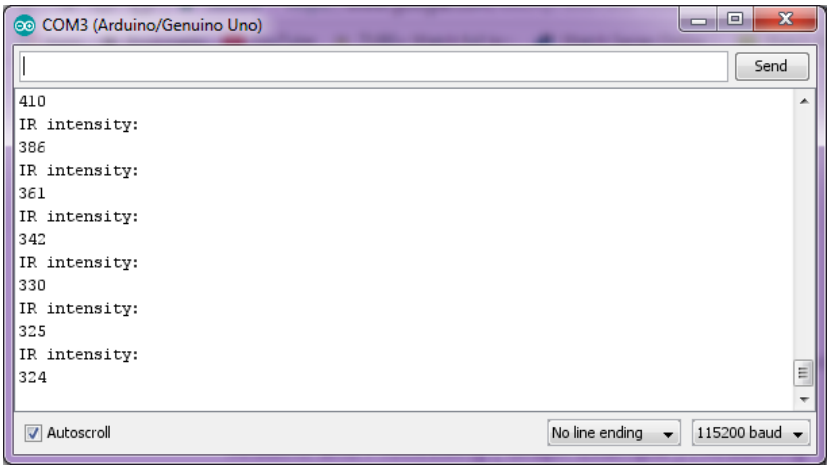

Figure 4.2.3: Output displayed using Serial Monitor

As shown in **Figure 4.2.2**, the output reading of the reflected IR emitter in AC signal is observed using Serial Monitor as the sensors is pressed against the skin. The amount of light absorbed by the arterial may change as the concentration of blood in artery varies. The small difference between the two wavelengths of Hb and HbO2 makes the value of the extinction coefficients is closely to each other which can cause the calculation of SpO_2 to be very sensitive to the measured value of R. To measure SpO_2 efficiently, a very accurate measurement of the PPG pulse amplitude is required.

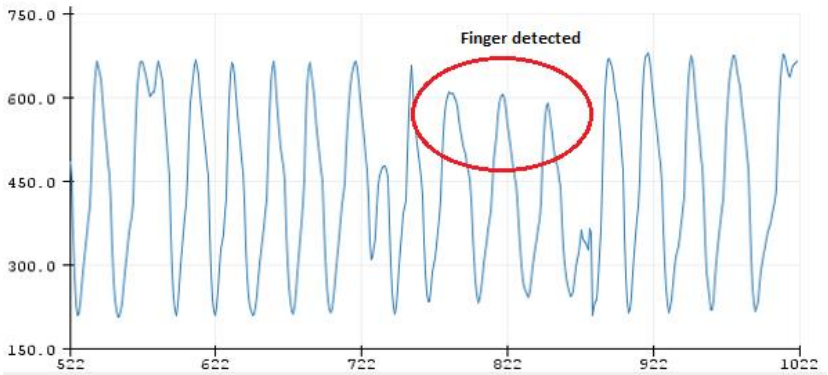

Figure 4.2.4: Output displayed using Serial Plotter

The PPG signal is seen to have formed a noticeable diastolic and systolic peak when a finger is placed against the sensing system. This is due to the increase and decrease of blood volume. The volume that increases with systole is also known as the “alternating current” (AC) compartment

in which the blood volume does not change with the cardiac cycle is known as the non-pulsatile compartment. Thus, this results in varying peak. When there is a finger, there will be less light being detected by the photodiode as the oxy-hemoglobin will absorb the lights. Hence, this will result in a voltage drop. However, oximeters are vulnerable to motions. As finger moves, light levels will change dramatically. Errors may occur if the finger is not placed properly to the sensing system. Thus, (SpO_2) is unable to measure correctly. Based on **Figure 4.2.4**, the red circles reflect the small errors.

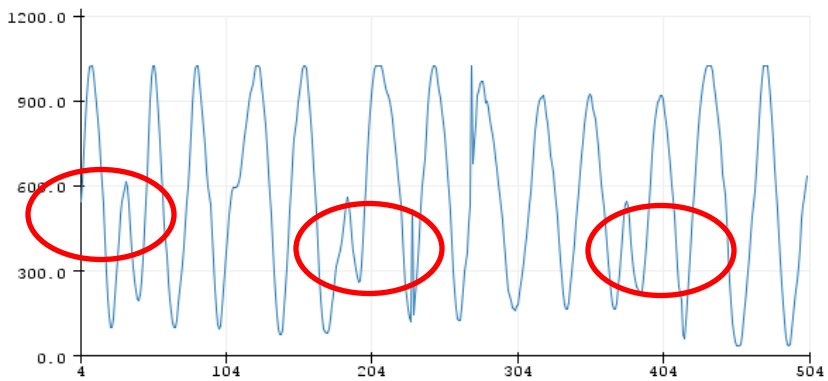

Figure 4.2.5: Output displayed after a few attempts

Plethysmography trace indicates how good the pulsatile signal is. If the characteristic of the pulsatile signal is very poor and unstable, it will result in wrong calculation of the oxygen saturation. The calculations to measure the oxygen saturation can be very complicated. Thus, obtaining the right signal is very important before determining the blood concentration.

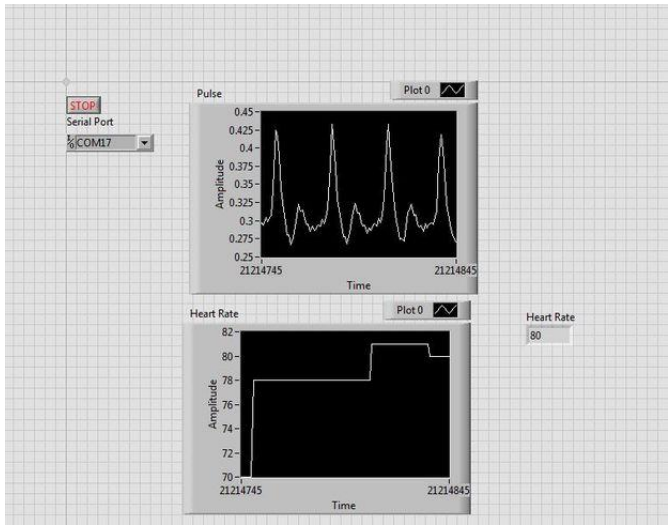

Figure 4.2.6: Simulation of pulsatile flow in arteries

The code reads the voltage from the circuit, which corresponds to the transmission of light through a person's finger. It then calculates the absorbance of the signal and outputs the data via serial communication. A corresponding LabVIEW VI reads the incoming serial data and plotted it with time. The resulting waveform is the pulse waveform. Thus, the oxygen saturation can be identified based on the pulse waveform obtained.

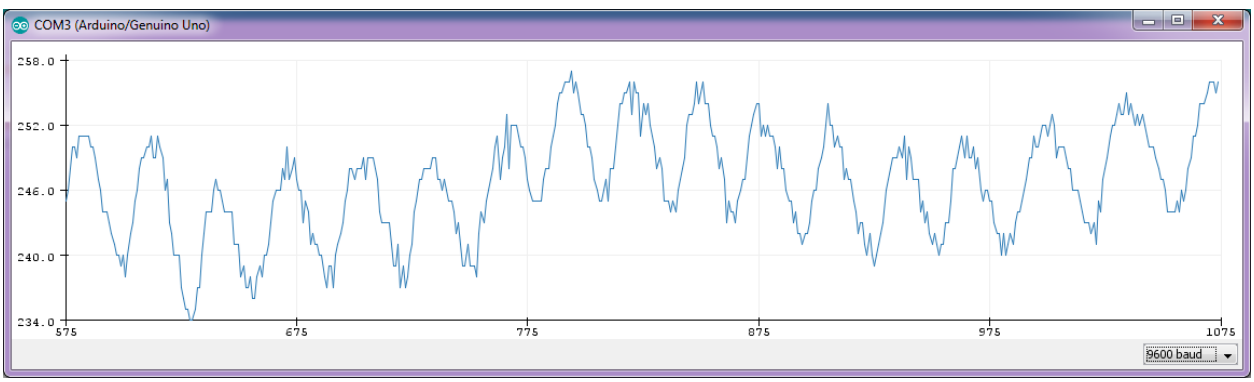

Figure 4.2.7: Testing (21/4/2017)

4.3 Estimation of SpO_2 Percentage

This section outlines the calculation of oxygen saturation SpO_2 using the PPG signal obtained based on **Figure 4.2.6**. The estimation relies on the relationship between the baseline value (DC) to the fluctuation in the signal (AC). The SpO_2 calculation is based on the pulse modulation

ratios in R which is defined in **Equation 2.7**. To avoid the PPG signal from contaminated, the op amp circuit helps to filter out the unwanted signal. This will ease in finding the measurement of SpO_2 properly. The ratio of ratios R for the sample PPG data is computed:

$$\boldsymbol{R = \frac{\left(\frac{AC_{red}}{DC_{red}}\right)}{\left(\frac{AC_{infrared}}{DC_{infrared}}\right)} = \frac{\left(\frac{4mV}{323mV}\right)}{\left(\frac{24mV}{920mV}\right)} = 0.455} \quad \textbf{(4)}$$

For the sample PPG data, the percentage of SpO_2 is determined as below:

$$\boldsymbol{SpO_2\% = 110 - 0.455 * 25 = 98.6\%} \quad \textbf{(5)}$$

The calculation made is based on the signal that has the most emphasized peaks and less noises. Somehow, every test conducted produced different Plethysmography trace. Therefore, for future work, multiple calibration needed to be done and compared so that the accuracy and precision of the system is identified.

4.4 Summary

Throughout the experimentation, the result obtained is based on the measuring site taken purely from a finger using the transmission method. The Plethysmography trace is formed and analyzed to determine the oxygen saturation SpO_2. The potential of variability in the result obtained is quite high and unpredictable. Therefore, some calculation made to measure the SpO_2 is inaccurate. Hence, the average reading must be identified from the comparison of the results based on the multiple calibrations made on the system to provide a precise measurement.

CHAPTER 5
CONCLUSION OF REPORT AND RECOMMENDATION

5.1 Overview of Conclusion and Recommendation

This chapter concludes all the findings from this research study. This can be one of the evidence that the development of the spectrophotometer is leading to a cost-effective product but still gives the similar output as the laser type. The summary will recap how this research manage to develop an optoelectronic device that uses the light-emitting diode (LED) as the source of light which function closely related to the laser therapy for a common treatment like neuropathy and brain stimulation but with safer, cost-saving and non-invasive technology. It is proven that the design can be built as a portable and lightweight device such that it would greatly increase the scope of possible applications of this technology in brain research. For future study, recommendation is included in this chapter.

5.2 Conclusion

The near infrared spectroscopy system is a powerful non-invasive method in imaging the brain activity and the measurement of cerebral oxygenation in biomedical application. The technology is of a great interest to most researchers out there and the medical profession, resulting in many clinical reviews related to neuroscience and physiology of exercise studies. By having the non-invasive system to be portable will makes it easy to handle providing a new direction of application for functional brain mapping.

Oximeter requires careful selection and implementation of a Transimpedance amplifier. This is to guarantee a correct conversion, distribution and processing of the input photocurrent. During calibration, optical sensors can be very sensitive in a way that even a slight movement could affect the reading. Thus, a proper probe is essential so that the photometric system works efficiently. Hence, determining the right pulsatile signal is important before moving to the next stage of measuring (SpO_2) .

For this project, the spectrophotometer technology is based on the development of a basic concept of NIRs system that optically measures the blood oxygenation of human tissue in most convenient and low cost technique while it is portable. Thus, the system is studied under literature review and is designed using the suitable specification is proven under the methodology section. In the end, the design must be applicable to detect the local hemodynamic response of the blood flow through tissues. With clinical collaboration, the system will be ready to imply successfully for monitoring the brain activities in detecting the mental stress.

5.3 Recommendation

5.3.1 Realistic Brain Phantom (Future Work)

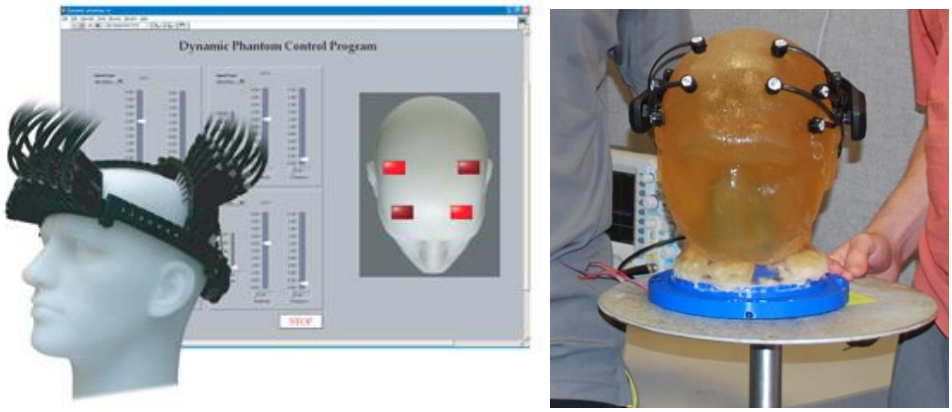

Figure 5.3.1 NIRs application tested on a brain phantom

To qualify the basic performance of the NIRs system in monitoring the brain activities, a test need to be done on a realistic brain phantom made from epoxy resin which is closely resembled to the actual brain tissues. The light source of the NIRs will be placed onto the phantom through a fiber-optic bundle to monitor the prefrontal cortex (PFC) located at the front side of the actual brain during the mental stress task**[20]**. The absorption and scattering coefficient in the blood-tissue is then analyzed to measure the concentration of cerebral oxygenation in order to identify the local hemodynamics response. The instrument used on the phantom need to be tested for a few times mainly for calibration purposes. The multiple result obtained based on the calibration will be used to identify the accuracy and precision of its performance. Thus, this will allow us to determine the next step of improving the system that might come in handy to the medical world in future.

Gantt Chart with Milestones

Activity	W1	W2	W3	W4	W5	W6	W7	W8	W9	W10	W11	W12	W13	W14
Create Design Specification														
Obtain Components Required for the Design Project														
Build Prototype														
Testing and Troubleshooting														
Submission of Progress Report								★						
Update Methodology and Result														
Improve and Modify Prototype														
Troubleshooting Test Execution														
Pre-SEDEX												★		
Submission of Draft Final Report													★	
Submission of Dissertation and Technical Report														★

★ Milestones

Benchmarking Study

REFERENCES

[1] S. J. Lupien and F. Seguin, "How to Measure Stress in Humans," Citeseer2007.

[2] P. Pinti, C. Aichelburg, F. Lind, S. Power, E. Swingler, A. Merla*, et al.*, "Using Fiberless, Wearable fNIRS to Monitor Brain Activity in Real-world Cognitive Tasks," p. e53336, Dec 2015.

[3] A. Bozkurt and B. Onaral, "Safety assessment of near infrared light emitting diodes for diffuse optical measurements," *BioMedical Engineering OnLine,* vol. 3, March 2004.

[4] M. A. Naeser and M. R. Hamblin, "Potential for Transcranial Laser or LED Therapy to Treat Stroke, Traumatic Brain Injury, and Neurodegenerative Disease," *Photomedicine and Laser Surgery,* vol. 29, pp. 443-446, 2011.

[5] N. Masataka, L. Perlovsky, and K. Hiraki, "Near-infrared spectroscopy (NIRS) in functional research of prefrontal cortex," *Frontiers in Human Neuroscience,* vol. 9, May 2015.

[6] A. Sakudo, "Near-infrared spectroscopy for medical applications: Current status and future perspectives," *Clinica Chimica Acta,* vol. 455, April 2016.

[7] M. N. Kim, T. Durduran, S. Frangos, B. L. Edlow, E. M. Buckley, H. E. Moss*, et al.*, "Noninvasive Measurement of Cerebral Blood Flow and Blood Oxygenation Using Near-Infrared and Diffuse Correlation Spectroscopies in Critically Brain-Injured Adults," *Neurocritical care,* vol. 12, pp. 173-180, 2010.

[8] S. K. Piper, A. Krueger, S. P. Koch, J. Mehnert, C. Habermehl, J. Steinbrink*, et al.*, "A wearable multi-channel fNIRS system for brain imaging in freely moving subjects," *NeuroImage,* vol. 85, Part 1, Jan 2014.

[9] T. Vaithianathan, I. D. Tullis, N. Everdell, T. Leung, A. Gibson, J. Meek*, et al.*, "Design of a portable near infrared system for topographic imaging of the brain in babies," *Review of scientific instruments,* vol. 75, pp. 3276-3283, 2004.

[10] R. G. Haahr, S. Duun, K. Birkelund, P. Raahauge, P. Petersen, H. Dam*, et al.*, "A Novel Photodiode for Reflectance Pulse Oximetry in low-power applications," in *2007 29th Annual International Conference of the IEEE Engineering in Medicine and Biology Society*, 2007, pp. 2350-2353.

[11] A. Aithal, "Wireless Sensor Platform for Pulse Oximetry," 2015.

[12] P. M. Mohan, A. A. Nisha, V. Nagarajan, and E. S. J. Jothi, "Measurement of arterial oxygen saturation $(\mathrm{SpO_2})$ using PPG optical sensor," in *2016 International Conference on Communication and Signal Processing (ICCSP)*, 2016, pp. 1136-1140.

[13] R. Nijland, H. W. Jongsma, J. Crevels, J. J. M. Menssen, J. G. Nijhuis, and B. Oeseburg, "Transmission Pulse Oximetry in the Fetal Lamb: Is There a Universal Calibration?," *Pediatr Res,* vol. 39, pp. 464-469, 03//print 1996.

[14] P. D. Mannheimer, J. Cascini, M. E. Fein, and S. L. Nierlich, "Wavelength selection for low-saturation pulse oximetry," *IEEE Transactions on Biomedical Engineering,* vol. 44, 1997.

[15] M. Nitzan, S. Noach, E. Tobal, Y. Adar, Y. Miller, E. Shalom*, et al.*, "Calibration-Free Pulse Oximetry Based on Two Wavelengths in the Infrared — A Preliminary Study," *Sensors (Basel, Switzerland),* vol. 14, pp. 7420-7434, 04/23/2014

[16] K. K. Tremper, "Pulse oximetry," *Chest Journal,* vol. 95, pp. 713-715, 1989.

[17] A. Kulcke, I. Menn, and A. Holmer, "Combining pulse oximetry and NIRS: Pulse Spectroscopy," 2012.

[18] K. Komiya, "Semiconductor integrated circuit supplying voltage to a load using a charge pump and electronic device including the same," ed: Google Patents, 2009.

[19] G. Palumbo, D. Pappalardo, and M. Gaibotti, "Charge-pump circuits: power-consumption optimization," *IEEE Transactions on Circuits and Systems I: Fundamental Theory and Applications,* vol. 49, pp. 1535-1542, 2002.

[20] M. Tanida, M. Katsuyama, and K. Sakatani, "Relation between mental stress-induced prefrontal cortex activity and skin conditions: a near-infrared spectroscopy study," *Brain research,* vol. 1184, 2007.

[21] G. Bauernfeind, R. Leeb, S. C. Wriessnegger, and G. Pfurtscheller, "Development, set-up and first results for a one-channel near-infrared spectroscopy system/Entwicklung, Aufbau und vorläufige Ergebnisse eines Einkanal-Nahinfrarot-Spektroskopie-Systems," *Biomedizinische Technik,* vol. 53, 2008.

[22] Jones, S., "Recent developments in near-infrared spectroscopy (NIRS) for the assessment of local skeletal muscle microvascular function and capacity to utilise oxygen." Artery Research 16:25-33, 2016.

[23] Kawano K., "Effects of sedative antidepressants on prefrontal cortex activity during verbal fluency task in healthy subjects: a near-infrared spectroscopy study." Psychopharmacology 226(1): 75-81, 2-13, 2015.

[24] Moghimi, S., "Automatic detection of a prefrontal cortical response to emotionally rated music using multi-channel near-infrared spectroscopy." Journal of neural engineering 9(2): pp. 26-22, 2012.

[25] Gateau, T., "Real-time state estimation in a flight simulator using fNIRS." PloS one 10(3): pp. 121-279, 2015.

[26] Pu, S., "The relationship between the prefrontal activation during a verbal fluency task and stress-coping style in major depressive disorder: a near-infrared spectroscopy study." Journal of psychiatric research 46(11): 1427-1434, 2012.

[27] Liu, T., "Appraisal of a copresent observer as supportive activates the left inferior parietal lobule: a near-infrared spectroscopy study using a driving video game." NeuroReport 23(14): 835-839, 2012.

[28] Jones, B., “The Use of Portable NIRS to Measure Muscle Oxygenation and Haemodynamics During a Repeated Sprint Running Test. Oxygen Transport to Tissue XXXV. S. Van Huffel, G. Naulaers, A. Caicedo, D. F. Bruley and D. K. Harrison. New York, NY, Springer New York: 185-191, 2013.

APPENDIX A

1. Arduino code

```
const int sensorPin = A0;
int sensorVal = 0;
unsigned long pulseCounter = 0;
unsigned long firstPulseStartTime = 0;
unsigned long secondPulseStartTime = 0;
unsigned long time_between_pulses = 0;
const unsigned long refractoryPeriod = 300;
const double minutes_in_milliseconds = 60000;
const double threshold = 0.33;
void setup()
{
 Serial.begin(115200);

 delay(2000); //a slight delay for system stabilization
}

void loop()
{
 //creates a timer variable to keep track of time
 unsigned long timer = millis();

 sensorVal = analogRead(sensorPin);
 double voltage = convertToVoltage(sensorVal);
 double absorbance = calculateAbsorbance(voltage);
 long time_between_pulses = detectThreshold(absorbance);
  int pulseRate = calculatePulseRate(time_between_pulses);
   displayPulseInLabVIEW(absorbance, pulseRate);

 //small delay to change our sampling rate
 //and stabilize our signal
 delay(25);
}

//displayPulseInLabVIEW()
//Outputs the data via serial communication. LabVIEW reads the
//data coming in and plots the pulse waveform as well as the
//pulse rate
void displayPulseInLabVIEW(double absorbance, int pulseRate)
{
 //Serial.print allows us to output the data
 //via serial communication
 Serial.print(absorbance,5);
 Serial.print("\t");
 Serial.print(pulseRate);
 Serial.println();
}
```

```
//convertToVoltage()
//Does the calculation to convert the Arduino's analog-to-digital
//converter number to a voltage. This function then returns the
//value to the rest of the program.
double convertToVoltage(double ADC_Val)
{
  double volt = 0;

  volt = 5*(ADC_Val/1023);

  return volt;
}
double calculateAbsorbance(double volt)
{
  double absorbance = 0;
  absorbance = log10(5/volt);
  return absorbance;
}

//calculatePulseRate()
//This method calculates pulse rate by dividing 60 seconds by the
//time between subsequent pulses
double calculatePulseRate(long time_between_pulses)
{
  return minutes_in_milliseconds/time_between_pulses;
}

//detectThreshold()
//This method detects whether the signal has passed our
//threshold and determines the time between subsequent peaks
long detectThreshold(double absorbance)
{
  if (millis() - firstPulseStartTime >= refractoryPeriod
    && absorbance >= threshold)
  {
    if (pulseCounter == 0)
    {
      pulseCounter++;
      firstPulseStartTime = millis();
    }
    else if (pulseCounter == 1)
    {
      secondPulseStartTime = millis();
      time_between_pulses = secondPulseStartTime -
firstPulseStartTime;
      firstPulseStartTime = secondPulseStartTime;
    }
  }
  return time_between_pulses;
}
```

2. Processing code

```
// Define signal parameters
int Sampling_Time = 5;
int Num_Samples = 600;
int Peak_Threshold_Factor = 80;
int Minimum_Range = 500;
int Minimum_Peak_Separation = 50;  // 50*5=250 ms
int Moving_Average_Num = 10;
int Index1, Index2, Index3, i, j, k, ZeroFlag;
float Pulse_Rate, Temp1, Peak1, Peak2, Peak3, PR1, PR2,
ADC_Range;
float Amplification_Factor,Peak_Magnitude, Peak_Threshold,
Minima, Range, temp, Sum_Points, Num_Points;
float[] ADC_Value = new float[Num_Samples];
int[] ADC_Index = new int[Num_Samples];
// Define display
float plotX1, plotY1;
float plotX2, plotY2;
float labelX, labelY;
int rowCount;
int columnCount;
int currentColumn = 0;
 int count = 0;
int yearMin, yearMax;
int[] years;

int xInterval = 10;
int yInterval = 200;

PFont plotFont;

import processing.serial.*;
Serial myPort;        // The serial port
void setup() {
  size(720, 450);
  plotX1 = 20;
  plotX2 = width - 20;
  labelX = 120;
  plotY1 = 50;
  plotY2 = height - 150;
  labelY = height - 100;
  plotFont = createFont("SansSerif", 20);
  textFont(plotFont);
  smooth();
  println(Serial.list());
  myPort = new Serial(this, Serial.list()[0], 115200);
  myPort.bufferUntil('\n');
}
```

```
void draw() {
  background(224);

  // Show the plot area as a white box
  fill(255);
  rectMode(CORNERS);
  noStroke();
  rect(plotX1, plotY1, plotX2, plotY2);
  drawTitle();
  drawAxisLabels();
  drawSampleLabels();
  ReadSamples();
  RemoveDC();
  if(ADC_Range < 50) {
    ZeroFlag = 1;
    ZeroData();
  } else ZeroFlag=0;
  ScaleData();
  FilterData();
  ComputeHeartRate();
  // draw the data using a long curve
  noFill();
  stroke(32, 128, 192);
  // balance the weight of the lines with the closeness of the data points
  strokeWeight(2);
  drawDataCurve();
  DisplayHeartRate();
  DisplayParameters();
}

void drawTitle() {
  fill(0);
  textSize(20);
  textAlign(LEFT);
  String title = "Easy Pulse PPG Analyzer V1.0";
  text(title, plotX1, plotY1 - 10);
}

void drawAxisLabels() {
  fill(0);
  textSize(16);
  textLeading(15);
  textAlign(CENTER);
  text("Samples  ("+nfc(Sampling_Time,  0)+"  ms)",  (plotX1+plotX2)/2,
labelY);
}

void drawSampleLabels() {
  fill(0);
  textSize(14);
  textAlign(CENTER);
```

```
  // Use thin, gray lines to draw the grid
  stroke(224);
  strokeWeight(1);

  for (int row = 0; row <= Num_Samples; row++) {
    if (row % 100 == 0) {
      float x = map(row, 0, Num_Samples+1, plotX1, plotX2);
      text(row, x, plotY2 + textAscent() + 10);
      line(x, plotY1, x, plotY2);
    }
  }
}

void ReadSamples(){
  count = 0;
  do{
    if(myPort.available() > 0){
      String inString = myPort.readStringUntil('\n');
      if (inString != null) {
        inString = trim(inString);
        float inByte = float(inString);
    //   float inByte = float(inString);
        ADC_Value[count] = inByte;
        ADC_Index[count] = count;
        count = count + 1;
      }
    }
  } while (count < Num_Samples);
}
void RemoveDC(){
  Find_Minima(0);
  Find_Peak(0);
  ADC_Range = Peak_Magnitude-Minima;
  println("Peak Magnitude2= "+ Peak_Magnitude + ", Minima = "+ Minima);
  println("Range of ADC_Samples= "+ Range);

  // Subtract DC (minima)
  for (int i = 0; i < Num_Samples; i++){
    ADC_Value[i] = ADC_Value[i] - Minima;
  }
  Minima = 0;  // New Minima is zero
}

void ZeroData(){
  for (int i = 0; i < Num_Samples; i++){
    ADC_Value[i] = 0;

  }
}
```

```
void ScaleData(){
 // Find peak value
 Find_Peak(0);
 Range = Peak_Magnitude - Minima;
 // Sclae from 1 to 1023
 for (int i = 0; i < Num_Samples; i++){
   ADC_Value[i] = 1 + ((ADC_Value[i]-Minima)*1022)/Range;

 }
 Find_Peak(0);
 Find_Minima(0);
 println("Peak Magnitude1= "+ Peak_Magnitude + ", Minima = "+ Minima);
}

void FilterData(){
 Num_Points = 2*Moving_Average_Num+1;
 for (i = Moving_Average_Num; i < Num_Samples-Moving_Average_Num; i++){
  Sum_Points = 0;
  for(k =0; k < Num_Points; k++){
   Sum_Points = Sum_Points + ADC_Value[i-Moving_Average_Num+k];
  }
 ADC_Value[i] = Sum_Points/Num_Points;
 }
 Find_Peak(Moving_Average_Num);
 Find_Minima(Moving_Average_Num);
 println("Peak Magnitude2= "+ Peak_Magnitude + ", Minima = "+ Minima);
}

void ComputeHeartRate(){

 // Detect Peak magnitude and minima
 Find_Peak(Moving_Average_Num);
 Find_Minima(Moving_Average_Num);
 println("Peak Magnitude3= "+ Peak_Magnitude + ", Minima = "+ Minima);
 Range = Peak_Magnitude - Minima;
 Peak_Threshold = Peak_Magnitude*Peak_Threshold_Factor;
 Peak_Threshold = Peak_Threshold/100;
 // Now detect three successive peaks
 Peak1 = 0;
 Peak2 = 0;
 Peak3 = 0;
 Index1 = 0;
 Index2 = 0;
 Index3 = 0;
 // Find first peak
 for (j = Moving_Average_Num; j < Num_Samples-Moving_Average_Num; j++){
    if(ADC_Value[j] >= ADC_Value[j-1] && ADC_Value[j] > ADC_Value[j+1] &&
      ADC_Value[j] > Peak_Threshold && Peak1 == 0){
       Peak1 = ADC_Value[j];
       Index1 = j;
    }
```

```
    // Search for second peak which is at least 10 sample time far
    if(Peak1 > 0 && j > (Index1+Minimum_Peak_Separation) && Peak2 == 0){
      if(ADC_Value[j] >= ADC_Value[j-1] && ADC_Value[j] > ADC_Value[j+1] &&
      ADC_Value[j] > Peak_Threshold){
        Peak2 = ADC_Value[j];
        Index2 = j;
      }
    } // Peak1 > 0

    // Search for the third peak which is at least 10 sample time far
    if(Peak2 > 0 && j > (Index2+Minimum_Peak_Separation) && Peak3 == 0){
      if(ADC_Value[j] >= ADC_Value[j-1] && ADC_Value[j] > ADC_Value[j+1] &&
      ADC_Value[j] > Peak_Threshold){
        Peak3 = ADC_Value[j];
        Index3 = j;
      }
    } // Peak2 > 0

  }
 PR1 = (Index2-Index1)*Sampling_Time; // In milliseconds
 PR2 = (Index3-Index2)*Sampling_Time;
 println("PR1 = "+PR1+", PR2 = "+PR2);
 if(PR1 > 0 && abs(PR1-PR2) < 100){
   Pulse_Rate = (PR1+PR2)/2;
   Pulse_Rate = 60000/Pulse_Rate; // In BPM
   println("Index2= "+ Index2 + ", Index1 = "+ Index1+", PulseRate= "+Pulse_Rate);
   println("Peak Magnitude= "+ Peak_Magnitude + ", Minima = "+ Minima);
 }
}

void drawDataCurve() {
  beginShape();
  if(ZeroFlag == 0){
   for (int row = Moving_Average_Num; row < Num_Samples-Moving_Average_Num; row++)
{
     stroke(32, 128, 192);
     float value = ADC_Value[row];
     float x = map(ADC_Index[row], 0, Num_Samples, plotX1, plotX2);
     float y = map(value, 0, Peak_Magnitude, plotY2, plotY1+15);
     if(row == Index1 || row == Index2 || row == Index3){
       textSize(20);
       text("x", x,y);
     }
     curveVertex(x, y);


    // if(row == Index2){
      //stroke(204, 102, 0);
     //  triangle(x,y-4, x-3, y+4, x+4, y+4 );
    // }
    // if(row == Index3){
      //stroke(204, 102, 0);
```

```
        //triangle(x,y-4, x-3, y+4, x+4, y+4 );
        //}
      }
    }
    else{
      for (int row = Moving_Average_Num; row < Num_Samples-Moving_Average_Num; row++) {
        float value = ADC_Value[row];
        float x = map(ADC_Index[row], 0, Num_Samples, plotX1, plotX2);
        float y = 200;
        curveVertex(x, y);
      }
    }
    endShape();
  }

  void DisplayHeartRate(){
    fill(200,0,0);
    textSize(20);
    textAlign(LEFT);
    text("BPM", plotX2-40, plotY1 - 10);
    if(ZeroFlag == 0){
      text(nfc(Pulse_Rate, 1), plotX2-100, plotY1 - 10);
    }else {
      text("000", plotX2-100, plotY1 - 10);
    }
  }
  void Find_Minima(int Num){
    Minima = 1024;
    for (int m = Num; m < Num_Samples-Num; m++){
        if(Minima > ADC_Value[m]){
          Minima = ADC_Value[m];
        }
    }
  }

  void Find_Peak(int Num){
    Peak_Magnitude = 0;
    for (int m = Num; m < Num_Samples-Num; m++){
        if(Peak_Magnitude < ADC_Value[m]){
          Peak_Magnitude = ADC_Value[m];
       }
    }
  }

  void DisplayParameters(){
    fill(250,00,00);
    textSize(18);
    textAlign(LEFT);
    text("Range of ADC Samples = "+ ADC_Range, plotX1+5, plotY2+80);
}
```

APPENDIX B

1. Red LED Datasheet

Kingbright

2.5x5mm RECTANGULAR SOLID LAMP

Part Number: L-383SRDT Super Bright Red

Features

- Low power consumption.
- Reliable and rugged.
- Excellent uniformity of light output.
- Suitable for level indicator.
- Long life - solid state reliability.
- RoHS compliant.

Description

The Super Bright Red source color devices are made with Gallium Aluminum Arsenide Red Light Emitting Diode.

Package Dimensions

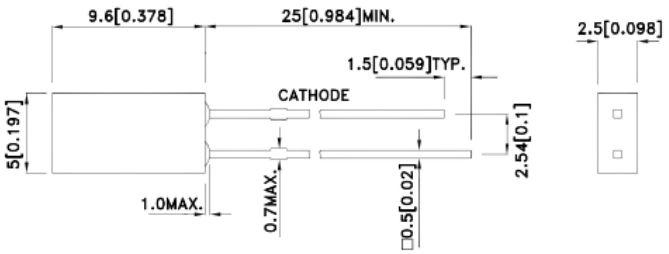

Notes:
1. All dimensions are in millimeters (inches).
2. Tolerance is ±0.25(0.01") unless otherwise noted.
3. Lead spacing is measured where the leads emerge from the package.
4. The specifications, characteristics and technical data described in the datasheet are subject to change without prior notice.

SPEC NO: DSAB4869	REV NO: V.8	DATE: APR/15/2010	PAGE: 1 OF 6
APPROVED: WYNEC	CHECKED: Allen Liu	DRAWN: Y.F.Lv	ERP: 1101003881

Kingbright

Selection Guide

Part No.	Dice	Lens Type	Iv (mcd) [2] @ 20mA		Viewing Angle [1]
			Min.	Typ.	2θ1/2
L-383SRDT	Super Bright Red (GaAlAs)	RED DIFFUSED	36	70	110°

Notes:
1. θ1/2 is the angle from optical centerline where the luminous intensity is 1/2 of the optical peak value.
2. Luminous intensity/ luminous Flux: +/-15%.

Electrical / Optical Characteristics at TA=25°C

Symbol	Parameter	Device	Typ.	Max.	Units	Test Conditions
λpeak	Peak Wavelength	Super Bright Red	660		nm	I_F=20mA
λD [1]	Dominant Wavelength	Super Bright Red	640		nm	I_F=20mA
Δλ1/2	Spectral Line Half-width	Super Bright Red	20		nm	I_F=20mA
C	Capacitance	Super Bright Red	45		pF	V_F=0V;f=1MHz
V_F [2]	Forward Voltage	Super Bright Red	1.85	2.5	V	I_F=20mA
I_R	Reverse Current	Super Bright Red		10	uA	V_R = 5V

Notes:
1.Wavelength: +/-1nm.
2. Forward Voltage: +/-0.1V.

Absolute Maximum Ratings at TA=25°C

Parameter	Super Bright Red	Units
Power dissipation	75	mW
DC Forward Current	30	mA
Peak Forward Current [1]	155	mA
Reverse Voltage	5	V
Operating/Storage Temperature	-40°C To +85°C	
Lead Solder Temperature [2]	260°C For 3 Seconds	
Lead Solder Temperature [3]	260°C For 5 Seconds	

Notes:
1. 1/10 Duty Cycle, 0.1ms Pulse Width.
2. 2mm below package base.
3. 5mm below package base.

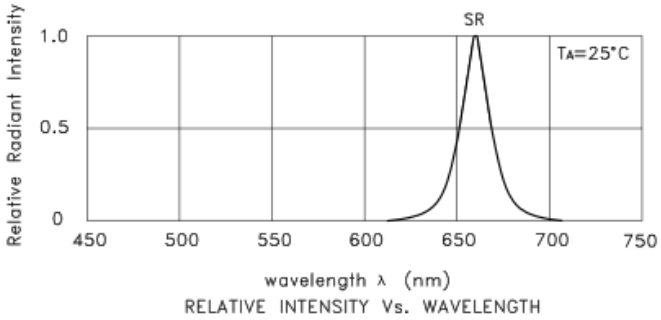

Super Bright Red **L-383SRDT**

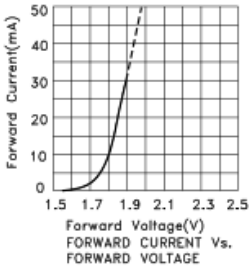

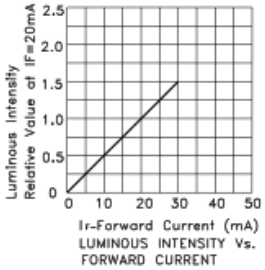

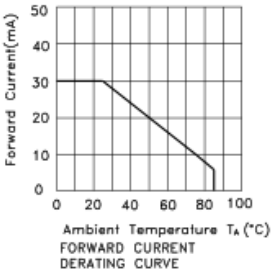

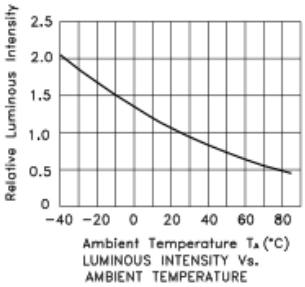

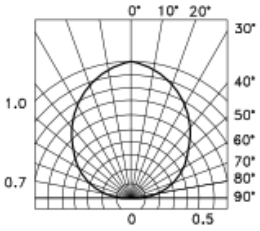

SPATIAL DISTRIBUTION

PACKING & LABEL SPECIFICATIONS **L-383SRDT**

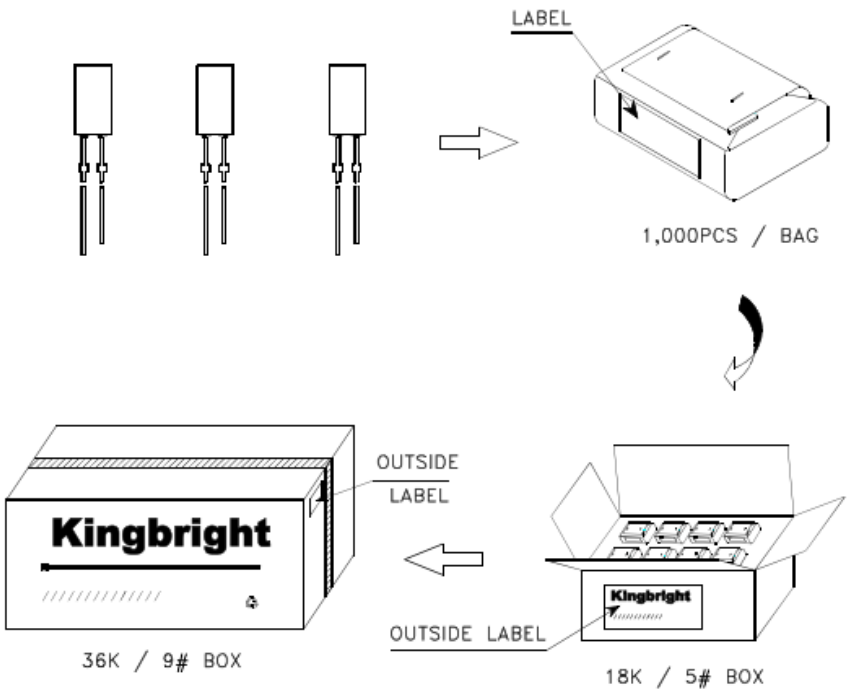

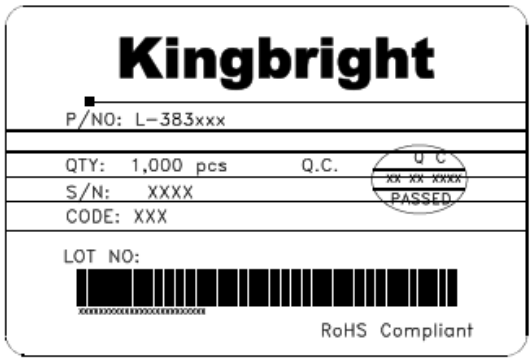

LED MOUNTING METHOD

1. The lead pitch of the LED must match the pitch of the mounting holes on the PCB during component placement. Lead-forming may be required to insure the lead pitch matches the hole pitch. Refer to the figure below for proper lead forming procedures.
(Fig. 1)

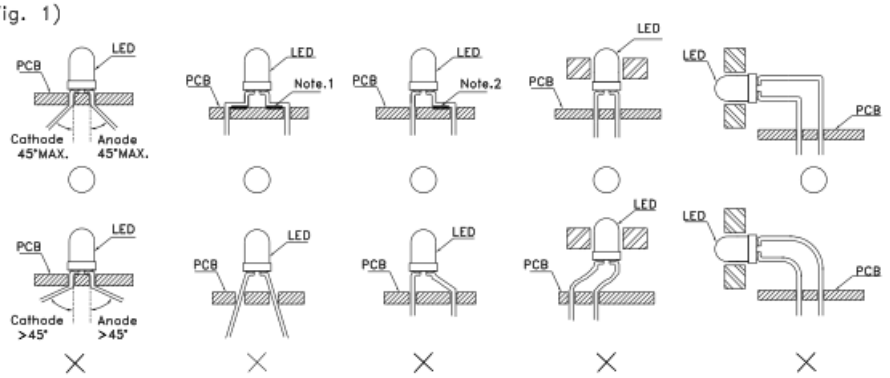

Fig.1

"○" Correct mounting method "×" Incorrect mounting method

Note 1-2 : Do not route PCB trace in the contact area between the leadframe and the PCB to prevent short-circuits.

2. When soldering wire to the LED, use individual heat-shrink tubing to insulate the exposed leads to prevent accidental contact short-circuit.
(Fig. 2)

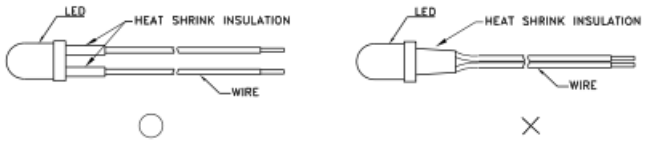

Fig. 2

3. Use stand-offs (Fig. 3) or spacers (Fig. 4) to securely position the LED above the PCB.

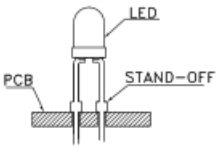

Fig. 3

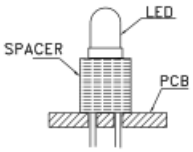

Fig. 4

LEAD FORMING PROCEDURES

1. Maintain a minimum of 2mm clearance between the base of the LED lens and the first lead bend. (Fig. 5 and 6)

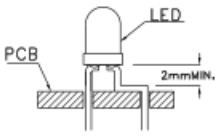

Fig. 5

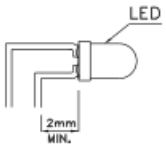

Fig. 6

2. Lead forming or bending must be performed before soldering, never during or after Soldering.
3. Do not stress the LED lens during lead-forming in order to fractures in the lens epoxy and damage the internal structures.
4. During lead forming, use tools or jigs to hold the leads securely so that the bending force will not be transmitted to the LED lens and its internal structures. Do not perform lead forming once the component has been mounted onto the PCB. (Fig. 7)
5. Do not bend the leads more than twice. (Fig. 8)

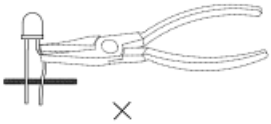

Fig. 7

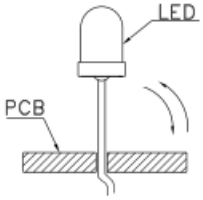

Fig. 8

6. After soldering or other high-temperature assembly, allow the LED to cool down to 50°C before applying outside force (Fig. 9). In general, avoid placing excess force on the LED to avoid damage. For any questions please consult with Kingbright representative for proper handling procedures.

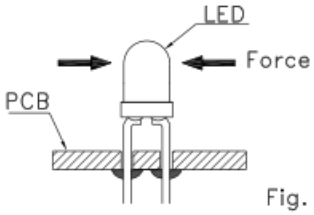

Fig. 9

2. Infrared LED Datasheet

Silicon PIN Photodiode with Daylight Blocking Filter
Silizium-PIN-Fotodiode mit Tageslichtsperrfilter
Version 1.0

SFH 235 FA

Features:
- Especially suitable for applications of 880 nm
- Short switching time (typ. 20 ns)
- 5 mm LED plastic package
- Also available on tape and reel

Besondere Merkmale:
- Speziell geeignet für Anwendungen bei 880 nm
- Kurze Schaltzeit (typ. 20 ns)
- 5 mm-Plastikbauform im LED-Gehäuse
- Auch gegurtet lieferbar

Applications
- Photointerrupters
- IR remote control of hi-fi and TV sets, video tape recorders, dimmers, remote controls of various equipment

Anwendungen
- Lichtschranken
- IR-Fernsteuerung von Fernseh- und Rundfunkgeräten, Videorecordern, Lichtdimmern, Gerätefernsteuerungen

Ordering Information
Bestellinformation

Type: **Typ:**	**Photocurrent** **Fotostrom** **λ = 870 nm, E_e = 1 mW/cm², V_R = 5 V** **I_P [µA]**	**Ordering Code** **Bestellnummer**
SFH 235 FA	50 (≥ 40)	Q62702P0273

OSRAM
Opto Semiconductors

Maximum Ratings (T_A = 25 °C)
Grenzwerte

Parameter Bezeichnung	Symbol Symbol	Values Werte	Unit Einheit
Operating and storage temperature range Betriebs- und Lagertemperatur	T_{op}; T_{stg}	-40 ... 100	°C
Reverse voltage Sperrspannung	V_R	32	V
Total power dissipation Verlustleistung	P_{tot}	150	mW

Characteristics (T_A = 25 °C)
Kennwerte

Parameter Bezeichnung	Symbol Symbol	Values Werte	Unit Einheit
Photocurrent Fotostrom (V_R = 5 V, E_e = 1 mW/cm^2, λ = 870 nm)	I_P	50 (≥ 40)	µA
Wavelength of max. sensitivity Wellenlänge der max. Fotoempfindlichkeit	$\lambda_{S\ max}$	900	nm
Spectral range of sensitivity Spektraler Bereich der Fotoempfindlichkeit	$\lambda_{10\%}$	740 ... 1120	nm
Radiant sensitive area Bestrahlungsempfindliche Fläche	A	7.02	mm^2
Dimensions of radiant sensitive area Abmessung der bestrahlungsempfindlichen Fläche	L x W	2.65 x 2.65	mm x mm
Half angle Halbwinkel	φ	± 65	°
Dark current Dunkelstrom (V_R = 10 V)	I_R	2 (≤ 30)	nA
Spectral sensitivity of the chip Spektrale Fotoempfindlichkeit des Chips (λ = 870 nm)	$S_{\lambda\ typ}$	0.65	A / W
Quantum yield of the chip Quantenausbeute des Chips (λ = 870 nm)	η	0.93	Electrons /Photon

Parameter Bezeichnung	Symbol Symbol	Values Werte	Unit Einheit
Open-circuit voltage Leerlaufspannung (E_e = 0.5 mW/cm², λ = 870 nm)	V_O	320 (≥ 250)	mV
Short-circuit current Kurzschlussstrom (E_e = 0.5 mW/cm², λ = 870 nm)	I_{SC}	22	µA
Rise and fall time Anstiegs- und Abfallzeit (V_R = 5 V, R_L = 50 Ω, λ = 850 nm, I_p = 800 µA)	t_r, t_f	0.02	µs
Forward voltage Durchlassspannung (I_F = 100 mA, E = 0)	V_F	1.3	V
Capacitance Kapazität (V_R = 0 V, f = 1 MHz, E = 0)	C_0	72	pF
Temperature coefficient of V_O Temperaturkoeffizient von V_O	TC_V	-2.6	mV / K
Temperature coefficient of I_{SC} Temperaturkoeffizient von I_{SC} (λ = 870 nm)	TC_I	0.03	% / K
Noise equivalent power Rauschäquivalente Strahlungsleistung (V_R = 10 V, λ = 870 nm)	NEP	0.039	pW / Hz$^{1/2}$
Detection limit Nachweisgrenze (V_R = 10 V, λ = 870 nm)	D^*	6.8e12	cm x Hz$^{1/2}$ / W

Relative Spectral Sensitivity
Relative spektrale Empfindlichkeit
$S_{rel} = f(\lambda)$

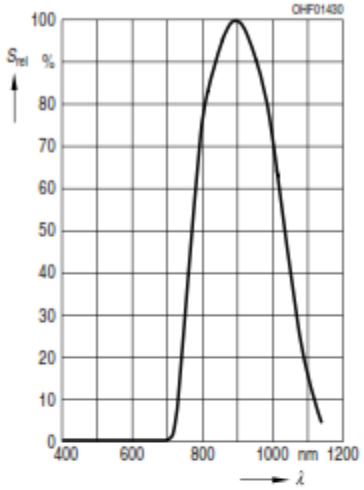

Photocurrent / Open-Circuit Voltage
Fotostrom / Leerlaufspannung
I_P (V_R = 5 V) / $V_O = f(E_e)$

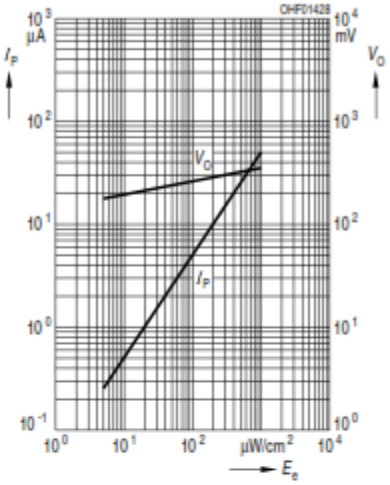

Total Power Dissipation
Verlustleistung
$P_{tot} = f(T_A)$

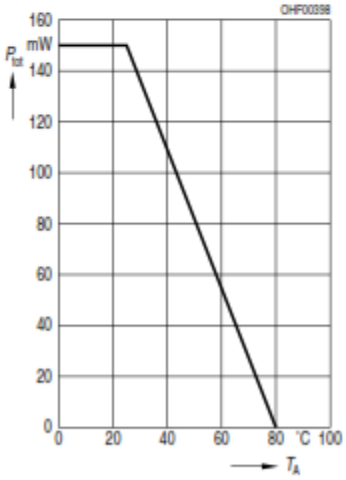

Dark Current
Dunkelstrom
$I_R = f(V_R)$, E = 0

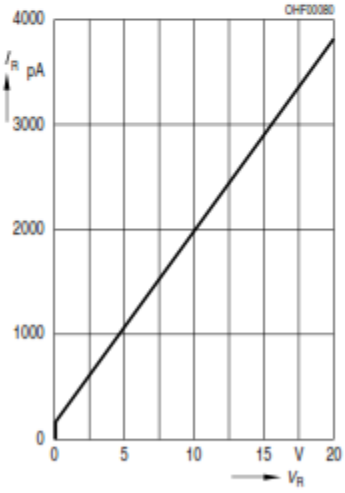

Capacitance
Kapazität
$C = f(V_R)$, f = 1 MHz, E = 0

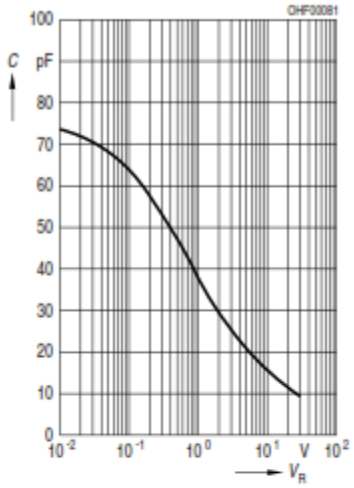

Dark Current
Dunkelstrom
$I_R = f(T_A)$, V_R = 10 V, E = 0

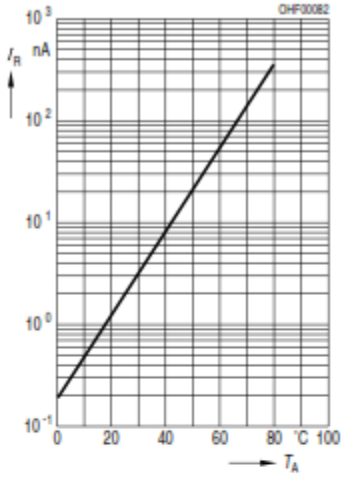

Directional Characteristics
Winkeldiagramm
$S_{rel} = f(\varphi)$

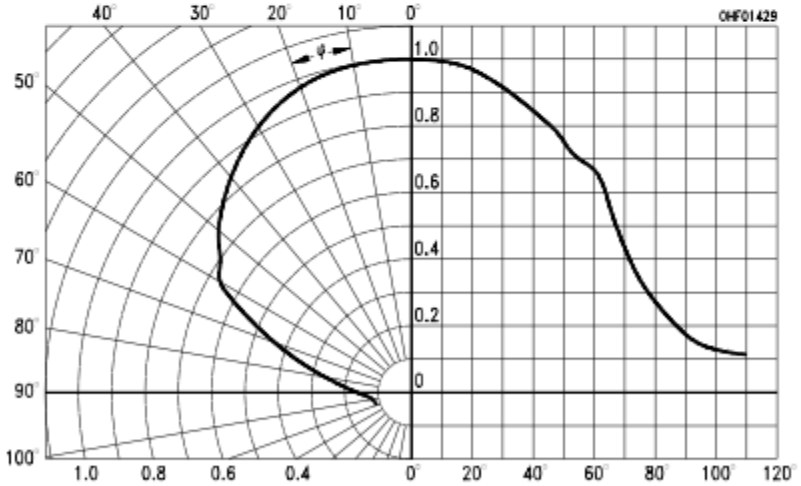

Package Outline
Maßzeichnung

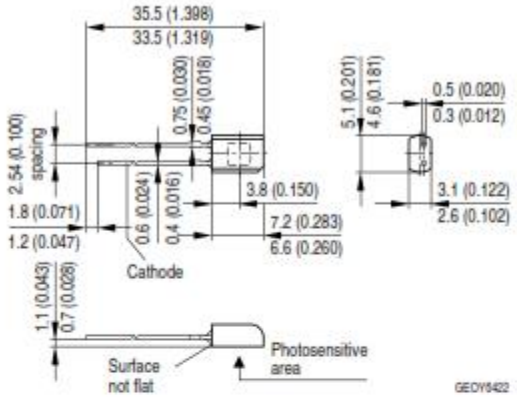

Dimensions in mm (inch). / Maße in mm (inch).

Package	5mm Radial (T 1 ¾), Epoxy
Gehäuse	5mm Radial (T 1 ¾), Harz

3. LM324N Datasheet

LM324, LM324A, LM324E, LM224, LM2902, LM2902E, LM2902V, NCV2902

Single Supply Quad Operational Amplifiers

The LM324 series are low−cost, quad operational amplifiers with true differential inputs. They have several distinct advantages over standard operational amplifier types in single supply applications. The quad amplifier can operate at supply voltages as low as 3.0 V or as high as 32 V with quiescent currents about one−fifth of those associated with the MC1741 (on a per amplifier basis). The common mode input range includes the negative supply, thereby eliminating the necessity for external biasing components in many applications. The output voltage range also includes the negative power supply voltage.

Features

- Short Circuited Protected Outputs
- True Differential Input Stage
- Single Supply Operation: 3.0 V to 32 V
- Low Input Bias Currents: 100 nA Maximum (LM324A)
- Four Amplifiers Per Package
- Internally Compensated
- Common Mode Range Extends to Negative Supply
- Industry Standard Pinouts
- ESD Clamps on the Inputs Increase Ruggedness without Affecting Device Operation
- NCV Prefix for Automotive and Other Applications Requiring Unique Site and Control Change Requirements; AEC−Q100 Qualified and PPAP Capable
- These Devices are Pb−Free, Halogen Free/BFR Free and are RoHS Compliant

ON Semiconductor®

www.onsemi.com

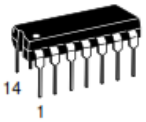

PDIP−14
N SUFFIX
CASE 646

SOIC−14
D SUFFIX
CASE 751A

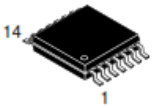

TSSOP−14
DTB SUFFIX
CASE 948G

PIN CONNECTIONS

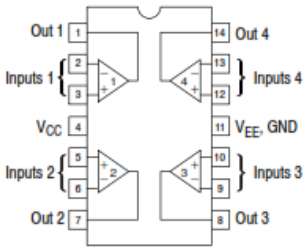

(Top View)

ORDERING INFORMATION

See detailed ordering and shipping information in the package dimensions section on page 10 of this data sheet.

DEVICE MARKING INFORMATION

See general marking information in the device marking section on page 11 of this data sheet.

MAXIMUM RATINGS (T_A = +25°C, unless otherwise noted.)

Rating	Symbol	Value	Unit
Power Supply Voltages Single Supply Split Supplies	 V_{CC} V_{CC}, V_{EE}	 32 ±16	Vdc
Input Differential Voltage Range (Note 1)	V_{IDR}	±32	Vdc
Input Common Mode Voltage Range	V_{ICR}	−0.3 to 32	Vdc
Output Short Circuit Duration	t_{SC}	Continuous	
Junction Temperature	T_J	150	°C
Thermal Resistance, Junction−to−Air (Note 2) Case 646 Case 751A Case 948G	$R_{\theta JA}$	118 156 190	°C/W
Storage Temperature Range	T_{stg}	−65 to +150	°C
Operating Ambient Temperature Range LM224 LM324, LM324A, LM324E LM2902, LM2902E LM2902V, NCV2902 (Note 3)	T_A	 −25 to +85 0 to +70 −40 to +105 −40 to +125	°C

Stresses exceeding those listed in the Maximum Ratings table may damage the device. If any of these limits are exceeded, device functionality should not be assumed, damage may occur and reliability may be affected.

1. Split Power Supplies.
2. All $R_{\theta JA}$ measurements made on evaluation board with 1 oz. copper traces of minimum pad size. All device outputs were active.
3. *NCV2902 is qualified for automitive use.*

ESD RATINGS

Rating	HBM	MM	Unit
ESD Protection at any Pin (Human Body Model − HBM, Machine Model − MM)			
NCV2902 (Note 3)	2000	200	V
LM324E, LM2902E	2000	200	V
LM324DG/DR2G, LM2902DG/DR2G	200	100	V
All Other Devices	2000	200	V

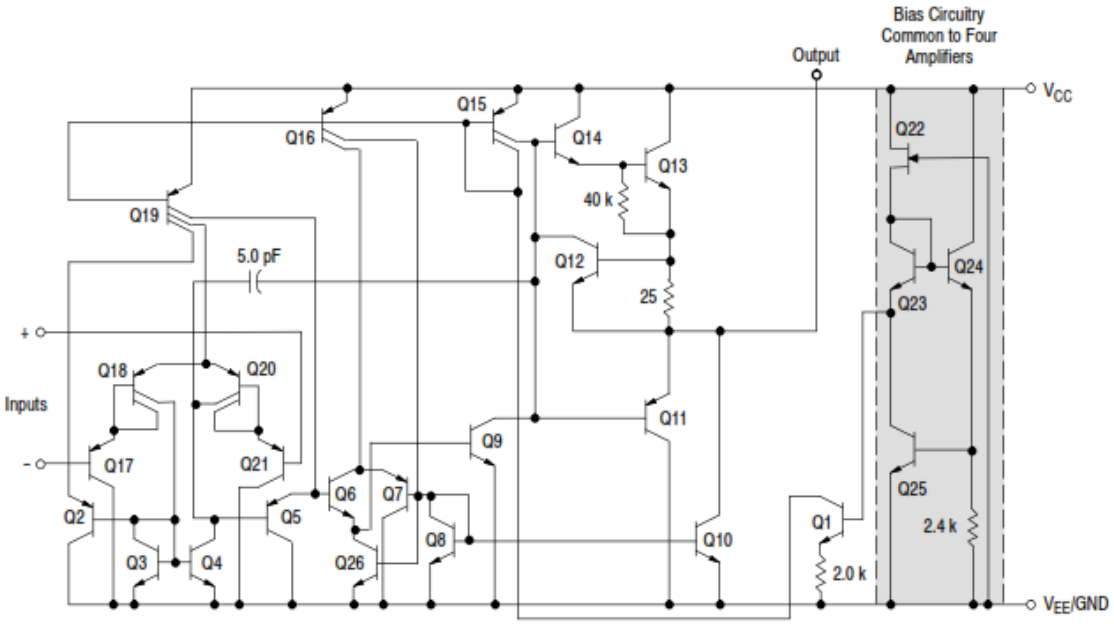

Figure 1. Representative Circuit Diagram
(One−Fourth of Circuit Shown)

CIRCUIT DESCRIPTION

The LM324 series is made using four internally compensated, two−stage operational amplifiers. The first stage of each consists of differential input devices Q20 and Q18 with input buffer transistors Q21 and Q17 and the differential to single ended converter Q3 and Q4. The first stage performs not only the first stage gain function but also performs the level shifting and transconductance reduction functions. By reducing the transconductance, a smaller compensation capacitor (only 5.0 pF) can be employed, thus saving chip area. The transconductance reduction is accomplished by splitting the collectors of Q20 and Q18. Another feature of this input stage is that the input common mode range can include the negative supply or ground, in single supply operation, without saturating either the input devices or the differential to single−ended converter. The second stage consists of a standard current source load amplifier stage.

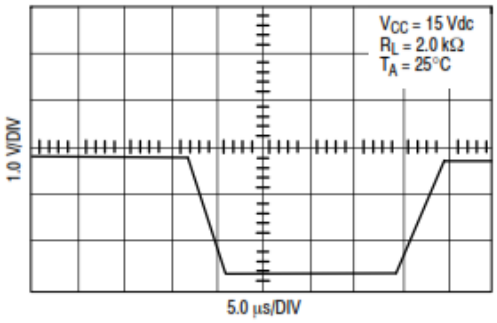

Figure 2. Large Signal Voltage Follower Response

Each amplifier is biased from an internal−voltage regulator which has a low temperature coefficient thus giving each amplifier good temperature characteristics as well as excellent power supply rejection.

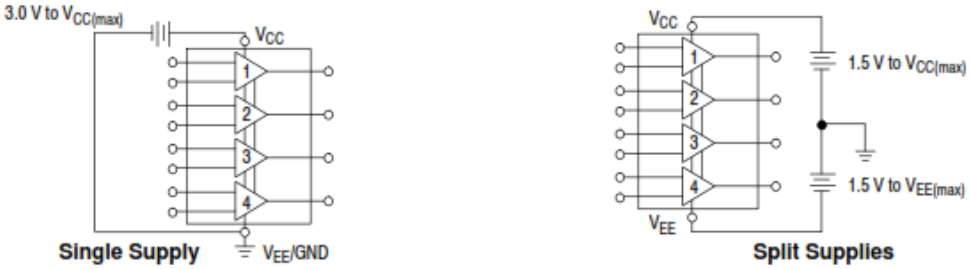

Figure 3.

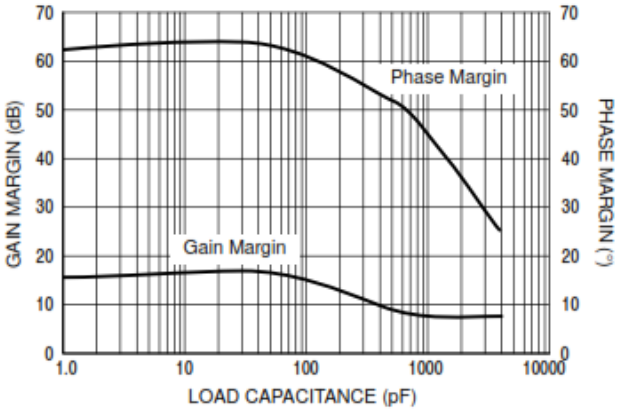

Figure 4. Gain and Phase Margin

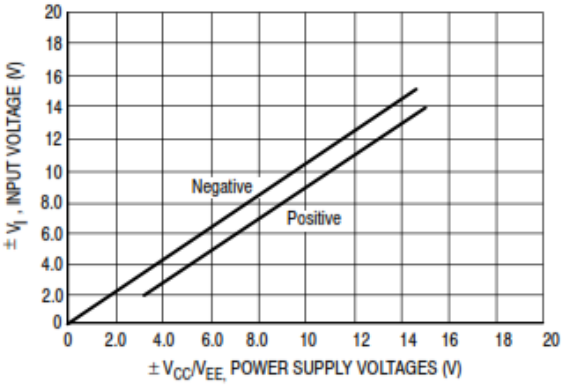

Figure 5. Input Voltage Range

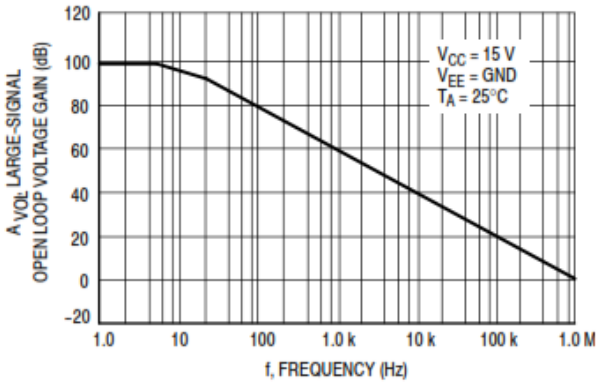

Figure 6. Open Loop Frequency

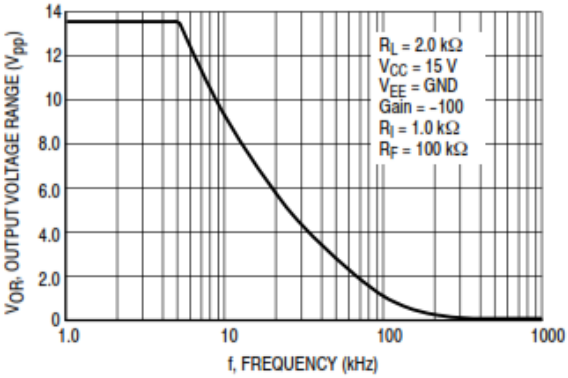

Figure 7. Large−Signal Frequency Response

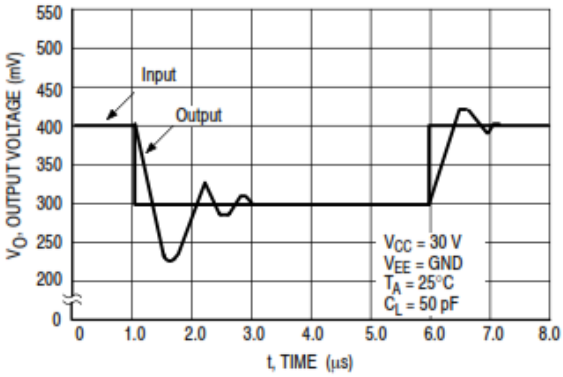

Figure 8. Small−Signal Voltage Follower Pulse Response (Noninverting)

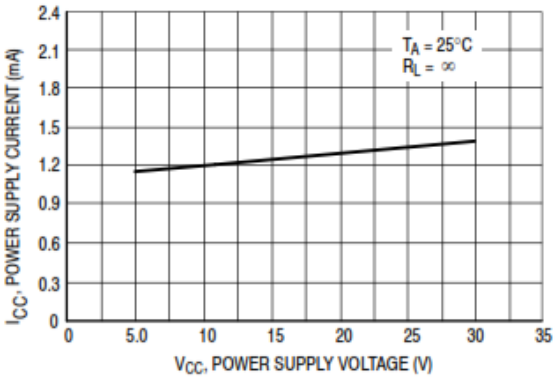

Figure 9. Power Supply Current versus Power Supply Voltage

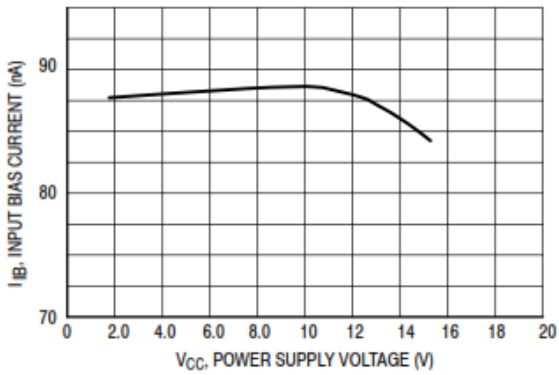

Figure 10. Input Bias Current versus Power Supply Voltage

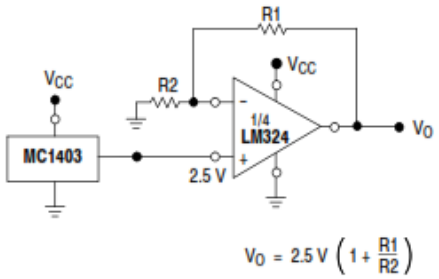

Figure 11. Voltage Reference

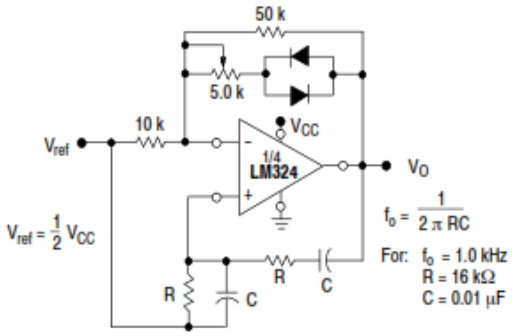

Figure 12. Wien Bridge Oscillator

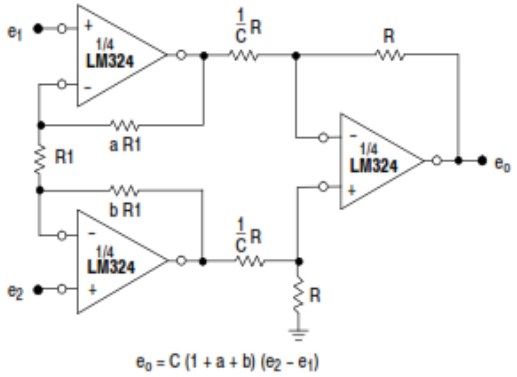

Figure 13. High Impedance Differential Amplifier

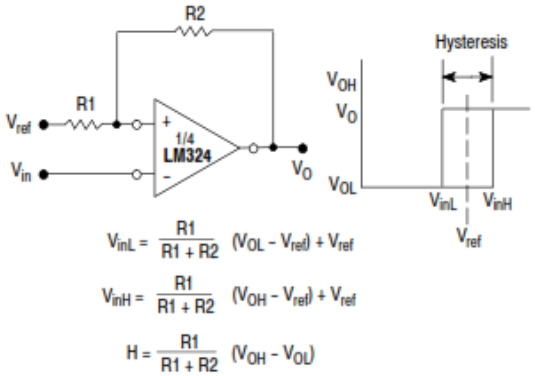

Figure 14. Comparator with Hysteresis

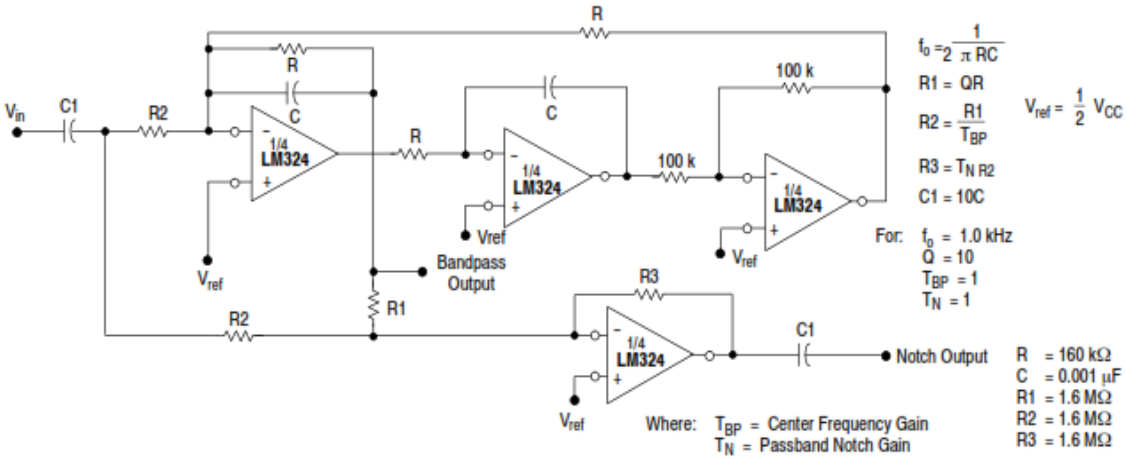

Figure 15. Bi−Quad Filter

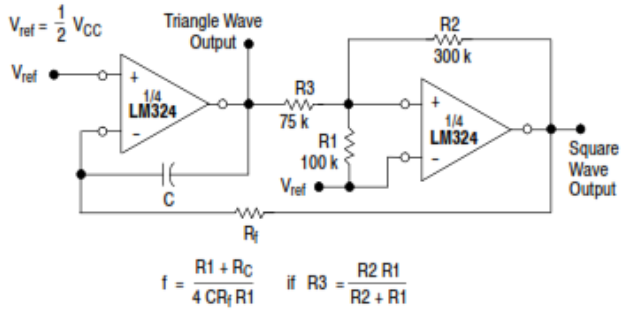

Figure 16. Function Generator

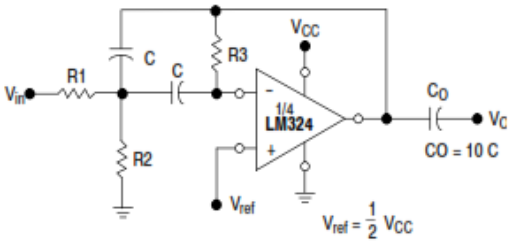

Figure 17. Multiple Feedback Bandpass Filter

Given: f_0 = center frequency
$A(f_0)$ = gain at center frequency

Choose value f_0, C

Then: $R3 = \frac{Q}{\pi f_0 C}$

$R1 = \frac{R3}{2 A(f_0)}$

$R2 = \frac{R1 R3}{4Q^2 R1 - R3}$

For less than 10% error from operational amplifier, $\frac{Q_0 f_0}{BW} < 0.1$

where f_0 and BW are expressed in Hz.

If source impedance varies, filter may be preceded with voltage follower buffer to stabilize filter parameters.